Diploma Thesis

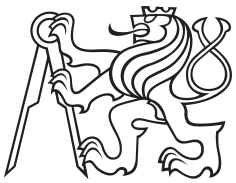

Czech Technical University in Prague

F3

Faculty of Electrical Engineering
Department of Control Engineering

Heat flow control of water-to-air heat exchanger

Ondřej Zlevor

Supervisor: Ing. Jiří Dostál
Field of study: Control Engineering
May 2017

Czech Technical University in Prague
Faculty of Electrical Engineering

Department of Control Engineering

DIPLOMA THESIS ASSIGNMENT

Student: **Zlevor Ondřej**

Study programme: Cybernetics and Robotics
Specialisation: Systems and Control

Title of Diploma Thesis: **Heat flow control of water-to-air heat exchanger**

Guidelines:

1. Study thermodynamics, distributed parameter systems and heat exchanger modeling
2. Prepare a simulation model of a heat exchanger and its test-bed setup. Focus on the heat exchanger model and its distributed parameter nature. Calibrate the model to the real test-bed if data is available.
3. Design a heat flow controller.
4. Test the proposed controller on the simulation model and the real test-bed if available..

Bibliography/Sources:

[1] Sandoval J.P. et. al. - Robust continuous velocity control of convective spatially distributed systems - Chemical Engineering Science 2008.
[2] Vouwer A.V. et. al. - Simulation of ODE/PDE Models with MATLAB, OCTAVE and SCILAB: Scientific and Engineering Applications - Springer 2014.
[3] Dostál J., Havlena V. - Convection Oriented Heat Exchanger Model - ICCA 2016.

Diploma Thesis Supervisor: Ing. Jiří Dostál

Valid until the summer semester 2017/2018

L.S.

prof. Ing. Michael Šebek, DrSc.
Head of Department

prof. Ing. Pavel Ripka, CSc.
Dean

Prague, November 30, 2016

Acknowledgements

I'd like to thank to everyone who has in any way helped me with the work related to this thesis. Above all, I want to thank my supervisor, Ing. Jiří Dostál, for his day-to-day support, for his scientific and teaching skills and patient guidance. Next big thanks belongs to my fellow students and collegues Jiří, Tomáš, Jan and Andrej, who remarkably helped with the testbed construction.

Declaration

I declare that the presented work was developed independently and that I have listed all sources of information used within it in accordance with the methodical instructions for observing the ethical principles in the preparation of university theses.

Prague, 23. May 2017

Abstract

This thesis is focused on heat flow control of a single phase water-to-air heat exchanger, where the manipulated variable is the water mass flow. First, a partial differential equation describing the heat exchanger was derived, then a state space simulation model was obtained by the Finite Volume Method, which was then used for tuning and testing of the control algorithms in Simulink. For the purposes of the heat flow and output water temperature control, two controllers were designed based on the controllers introduced by Shang [15] and by Sandoval [8].

A testbed representing a single heat exchanger one-pipe hydronic system was build to test the controllers within a real process. The experiments were run as a hardware-in-the-loop simulations, where Arduino on the testbed side communicates via serial line with Simulink. Finally, through several experiments we demonstrate the control performance improvement due to utilization of the proposed controllers.

Keywords: heat flow, heat exchanger, hydronic heating system

Supervisor: Ing. Jiří Dostál
Department of Control Engineering,
Karlovo náměstí 13,
Praha 2

Abstrakt

Tato práce se zabývá řízením tepelného toku v jednofázovém tepelném výměníku voda-vzduch, kdy řízeným vstupem je hmotnostní tok vody. Nejprve byla odvozena parciální diferenciální rovnice popisující tepelný výměník, následně se metodou konečných objemů získal stavový popis systému, který byl posléze využit pro ladění a testování řídicích algoritmů v Simulinku. Pro účely řízení teploty výstupní vody a tepelného toku byly použity dva regulátory podle regulátorů navržených Shangem [15] a Sandovalem [8].

Aby bylo možné otestovat regulátory i v reálném světě, byl postaven testbed, který reprezentuje jednotrubkový otopný systém s jedním tepelným výměníkem. Experimenty prováděné na testbedu měly formu hardware-in-the-loop testů, ve kterých Arduino na straně testbedu komunikovalo se simulací v Simulinku přes sériovou linku. Na vykonaných experimentech se ukázáno zlepšení výsledků řízení při použití představených regulátorů.

Klíčová slova: tepelný tok, tepelný výměník, otopný systém

Překlad názvu: Řízení tepelného toku výměníkem

Contents

Figures

Tables

List of Symbols

Constants

c_p	Water specific heat capacity at constant pressure	$[\mathrm{J\,kg^{-1}\,K^{-1}}]$
ρ_w	Water density	$[\mathrm{kg\,m^{-3}}]$

Heat exchanger

C_b	Heat capacity of heat exchanger body	$[\mathrm{J\,K^{-1}}]$
C_w	Heat capacity of water in heat exchanger	$[\mathrm{J\,K^{-1}}]$
$LMTD$	Logarithmic mean temperature difference	
$\dot{m}$	Mass flow	$[\mathrm{kg\,h^{-1}}]$
Q	Heat flow	[W]
Θ	Unused water heat content	
UA	Heat transfer rate	$[\mathrm{W\,K^{-1}}]$
x	Normalized spatial position in heat exchanger	

Temperatures

$T(x,t)$	Water temperature in spatial point x
T_{ai}	Inlet air temperature
T_{bi}	Boiler inlet water temperature
T_{bo}	Boiler outlet water temperature
$\langle T \rangle$	Mean water temperature
T_{wi}	HX inlet water temperature
T_{wo}	HX outlet water temperature
$T_{wo.SP}$	Outlet water temperature set-point

Chapter 1

Introduction

It is said that control of fire was the essential milestone in the human evolution. To our ancestors there were several important things provided through fire and one of them was heat. Since that time humans were able to heat their habitations. Even that heating is known for hundred of thousands of years there is still a lot of space for improvement. During the last century households got rid of dependency on solid fuel and started to use much cleaner and more comfortable heat sources such as electricity or natural gas.

The challenges brought by the 21st century are to decrease the heating costs while keeping or increasing the level of comfort by the usage of smart control of heating systems. Nowadays the hydronic heating is widespread; Fluid (usually water) is heated up in a boiler, next, the hot fluid gets transported to the heat exchanger where it transmits its heat to the surrounding area and finally the fluids flows back to boiler to repeat the cycle.

The hydronic heating system, as we understand it now, was first put into service in the Summer Palace in St. Petersburg in 1710 and became an inspiration for similar systems in other countries. However, in those days no electrical pump was known, so the water circulation was only gravitational, which brought strict requirements for the system construction and limited its usage. In virtue of that the heating systems with a steam as a working medium came to usage. This system was first build in England in 1832 and it soon became very popular, because the steam flow was induced by a pressure in the boiler. On the other hand such a system was very dangerous and had a high failure rate. In 1855, the first cast iron column radiator was invented, which has been the most popular radiator type till today.

The heating system control progress accelerated during the WW I, due to the lack of

coal and government initiative the automatic system development got a push. The first coal stokers controlled by thermostat appeared on market in 1912. During the 1920s, gas became to be widely used for heating, which also contributed to better control possibilities. During the 20th century, due to the expansion of electrical circulators, there came a divert from a bulky cast iron radiators to the low profile baseboard heating convectors. Nevertheless, no big change in the hydronic system control occured until balancing was an issue. In order to solve this, a Pressure Independent Control Valves (PICVs) were developed. It helped to distribute water in the hydronic systems effectively. Nowadays, there is a trend of inclination towards a utilization of pump driven systems. By this solution, the balancing is not issue anymore and it offers added values as hydronic system monitoring (e.g. heat metering, advanced optimization without further instruments).

1.1 Motivation

The aim of heating is to provide a cosy environment in a room. There are many rooms in a building and not all occupants of the building have the same temperature demands. The aim of the smart heating control is to provide a cosy environment for every single room in the building, while every room can hold a different temperature, while every room has different thermal properties and while there is only a one heat source for the whole building. Hence it is not possible to achieve this only by manipulating the boiler power.

Why not to do it smartly? If there is a model of the building, one can estimate the heat flows leaving or entering the thermal zones and it is possible to compute the needed heat flows, which have to be provided by radiators, to reach the temperature set-points. But then it is necessary to be able to control the radiator/heat exchanger heat flow. The heat flow can be estimated from knowledge of a difference between temperatures of the inlet and outlet water and a water mass flow. It is not a big problem to place a thermal sensors in a radiator and nor it is very expensive. On the other hand, to install a flow-meter to every radiator would significantly increase cost of this solution. Fortunately, several pumps in the market enable measurement of the rotational speed and with the supply current measurement, one can successfully estimate the mass flow (subject of the diploma thesis of J. Valtr [18]).

1.2 Scientific research

A heat exchanger heat flow control is a problem of controlling a transport delay dynamical system with distributed parameters described by a First-Order Partial Differential

Equations (FOPDEs). Several techniques were already developed and used to solve such a problem. The feedback control of a hyperbolic Partial Differential Equation (PDE) system was described by Christofides in [4]. It involves breaking the system into a set of Ordinary Differential Equations (ODEs) by utilization of the Galerkin's method. He also introduced a robust control of such a system. In other works, the sliding mode control was used. Sira-Ramirez [17] introduced a sliding mode control of dynamic nonlinear systems. This controller was modified by Hanczyc and Palazoglu [9], who used the Method of characteristics to get a system of ODEs describing the FOPDE system and define a sliding mode control of a spatial temperature profile in a heat exchanger. Shang [15] altered the Hanczyc controller and added an integral part to it to get better output response.

All these approaches require prior knowledge of some system parameters. Pourkargar and Armaou [2] combine Galerkin's method and proper ortogonal decomposition to generate a reduced order model, which roughly catches the model behavior and then serves as a basis for a Lyapunov-base adaptive controller design. Sandoval [8] developed a framework for design of robust controllers of FOPDE systems with time varying uncertain variables. The system input is the characteristic flow velocity and the output can be any variable, which depends on the states at a single axial point.

Subject of this diploma thesis is control of heat exchanger; The controlled output is either the outlet water temperature or the heat flow. Both the Sandoval's and the Shang's controllers were implemented and tested by a simulation in a Simulink environment and then on a testbed, which was build for this purpose. The second chapter explains a mathematical description of heat exchanger, its modelling and a couple of properties used for control and simulation purposes. In the third chapter, construction of the testbed is introduced in detail. In the fourth chapter, the control laws are derived and then the results of the simulations and testbed experiments are presented in the last chapter.

Chapter 2

Heat Exchanger Model

2.1 PDE representation

A heat exchanger, which is used as an object of this thesis, can be thought of as a metal tube filled with a flowing liquid. During the time the liquid spends in the tube, a part of its heat is conveyed to the tube and from there to the surrounding air. A Heat Exchanger (HX) is a distributed parameter system so it is not possible to describe it by a set of Ordinary Differential Equations (ODE), but it can be represented by a transport Partial Differential Equation (PDE). If we consider a unit length exchanger tube, then such a PDE can be derived from a formula describing a heat increase of the heat exchanger as

$$\frac{\partial}{\partial t}\int_0^1 T(x,t)\, c_p\, A\, \rho_w dx = \dot{m}\, c_p\, (T(0,t) - T(1,t)) - UA\int_0^1 (T(x,t) - T_{ai}(t))\, dx\ . \quad (2.1)$$

$T(x,t)$ [°C] is the water temperature along the heat exchanger normalized longitudinal coordinate x The left side of Eq. (2.1) represents a time-change of heat, which is stored in the water in HX, where c_w [J kg^{-1} K^{-1}] is the specific heat capacity of water, A [m^2] is the cross-sectional area of the HX tube and ρ_w [kg m^{-3}] is the water density. The first expression on the right side represents a difference between the heat flow transported in and out of the tube by the flowing water, where $T(0,t)$[°C] is a temperature of the incoming water and $T(1,t)$ [°C] of the leaving water. It could be also understood as

$$\dot{m}\, c_p\, (T(0,t) - T(1,t)) = -\dot{m}\, c_p \int_0^1 \frac{\partial T}{\partial x} dx. \quad (2.2)$$

The last expression is a heat flow between the heat exchanger and the surrounding air, where T_{ai} [°C] is the surrounding air temperature. It involves also the neglected dynamics of the heat exchanger body. After differentiation of Eq.(2.1) with respect to x, we get a partial differential equation Eq.(2.3) describing the heat exchanger

$$\frac{\partial T(x,t)}{\partial t} c_p \, A \, \rho_w = -\dot{m}(t) \, c_p \frac{\partial T(x,t)}{\partial x} - UA \, (T(x,t) - T_{ai}) \ . \tag{2.3}$$

To get a complete system description we have to add a boundary condition (BC) T_{wi}, the initial condition (IC) $T(x,0)$ and a system output T_{wo}, to finally get

$$\begin{aligned} &\frac{\partial T(x,t)}{\partial t} c_p \, A \, \rho_w + \dot{m}(t) \, c_p \frac{\partial T(x,t)}{\partial x} + UA \, (T(x,t) - T_{ai}) = 0, \ T(x,0) = T_0(x) \\ &T(0,t) = T_{wi}(t), \\ &T(1,t) = T_{wo}(t). \end{aligned} \tag{2.4}$$

2.2 Heat exchanger properties and relations

This section explains some properties and relations of the heat exchanger, which are used in following chapters.

2.2.1 UA estimation

Some of the used controllers require knowledge of the heat transfer coefficient. It is possible to identify this parameter from steady-state values of T_{wi}, T_{wo}, T_{ai} and $\dot{m}$. In the steady-state the heat flow can be found by two approaches, from the heat transfer between the hot water and cool air as

$$Q = UA \, (\langle T \rangle - T_{ai}) \tag{2.5}$$

or from heat lost by the fluid during the time spent in the heat exchanger as

$$Q = \dot{m} c_p \, (T_{wi} - T_{wo}) \, . \tag{2.6}$$

The value of $\langle T \rangle$ is found according to Eq. (2.18) (explained in the following text) and the heat transfer coefficient is

$$UA = \frac{\dot{m} c_p \, (T_{wi} - T_{wo})}{\langle T \rangle - T_{ai}}. \tag{2.7}$$

2.2.2 $\langle T \rangle$ estimation

Some of the controllers described in this paper utilize a mean value of the temperature profile $\langle T \rangle$ in the heat exchanger. It is physically not possible to measure the temperature along the whole heat exchanger and to compute the mean value from that. In steady state, however, the value of $\langle T \rangle$ can be estimated from temperatures T_{wi} and T_{wo}.

In a steady-state the time derivative of the temperature profile is zero

$$\frac{\partial T(x,t)}{\partial t} = 0, \tag{2.8}$$

and so the Eq. (3.14) reduces to an ODE

$$\begin{aligned} \dot{m}c_p \frac{\partial T(x)}{\partial x} &= -UA\left(T(x) - T_{ai}\right) \\ T(0) &= T_{wi}\ . \end{aligned} \tag{2.9}$$

Solution of Eq. (2.9) describing the spatial distribution of temperature $T(x) = T(\infty, x)$ is

$$T(x) = T_{ai} + \left(T_{wi} - T_{ai}\right) e^{-\alpha x}\ , \tag{2.10}$$

where $\alpha = \frac{UA}{\dot{m}c_p}$. Let's transform 2.10 into

$$\frac{T(x) - T_{ai}}{T_{wi} - T_{ai}} = e^{-\alpha x} \tag{2.11}$$

and let's define the unused water heat content $\Theta(x)$ along the x coordinate as

$$\Theta(x) = \frac{T(x) - T_{ai}}{T_{wi} - T_{ai}} = e^{-\alpha x}. \tag{2.12}$$

The mean value of $\Theta(x)$ along the x coordinate is

$$\begin{aligned} \langle \Theta \rangle = \int_0^1 \Theta(x)dx = \int_0^1 e^{-\alpha x}dx = \\ -\frac{1}{\alpha}\left[e^{-\alpha x}\right]_0^1 = -\frac{1}{\alpha}\left(e^{-\alpha} - 1\right) = \frac{1}{\alpha}\left(1 - \Theta(1)\right). \end{aligned} \tag{2.13}$$

The unknown parameters $\Theta(1)$ and α are determined from Eq. (2.37) as

$$\Theta(1) = \frac{T_{wo} - T_{ai}}{T_{wi} - T_{ai}} \tag{2.14}$$

$$\alpha = -ln\Theta(1). \tag{2.15}$$

From Eq. (2.37) we get according to properties of the mean value

$$\langle \Theta \rangle = \left\langle \frac{T(x) - T_{ai}}{T_{wi} - T_{ai}} \right\rangle = \frac{\langle T \rangle - T_{ai}}{T_{wi} - T_{ai}} \tag{2.16}$$

and the searched mean value of $T(x)$ is

$$\langle T \rangle = \langle \Theta \rangle \left(T_{wi} - T_{ai} \right) + T_{ai}. \tag{2.17}$$

Let's mark $\Theta_{out} = \Theta(1)$ and after substitution for $\langle \Theta \rangle$ from Eq. (2.13) and Eq. (2.15), we get

$$\langle T \rangle = \frac{-1}{ln\Theta_{out}} \left(1 - \Theta_{out} \right) \left(T_{wi} - T_{ai} \right) + T_{ai}, \tag{2.18}$$

which can be transformed as

$$\langle T \rangle = \frac{\frac{T(x)-T_{ai}}{T_{wi}-T_{ai}} - 1}{\ln\left(\frac{T(x)-T_{ai}}{T_{wi}-T_{ai}}\right)} \left(T_{wi} - T_{ai} \right) + T_{ai} \tag{2.19}$$

$$= \frac{T_{wo} - T_{ai} - T_{wi} + T_{ai}}{\ln\left(\frac{T(x)-T_{ai}}{T_{wi}-T_{ai}}\right)} + T_{ai} = LMTD + T_{ai}, \tag{2.20}$$

where $LMTD$ is the *Logarithmic mean temperature difference* (expressed more in detail in the following text).

2.2.3 T_{wo} reference computation from heat flow reference

The heat flow depends among others also on the outlet water temperature T_{wo}, which can be measured easily. It makes it suitable to use it as the controlled output. If we want to control the heat flow Q, we can reform the set-point Q_{SP} into the outlet water temperature set-point $T_{wo.SP}$ and instead of controlling the heat flow, control the output temperature. The way how to do it is described in this section.

Constant UA

Let's start with the relation between the outlet water temperature and the heat flow

$$Q = \dot{m} c_p \left(T_{wi} - T_{wo} \right) \ , \tag{2.21}$$

where $\dot{m}$ [$\mathrm{kg\,s^{-1}}$] is the water mass flow, c_p [$\mathrm{J\,kg^{-1}\,K^{-1}}$] the water specific heat capacity at constant pressure, T_{wi} [°C] and T_{wo} [°C] are temperatures of water at the beginning and at the end of the heat exchanger respectively. We can try to simply express the $T_{wo.SP}$ from Eq. (2.21) as

$$T_{wo.SP} = -\frac{Q}{\dot{m} c_p} + T_{wi}. \tag{2.22}$$

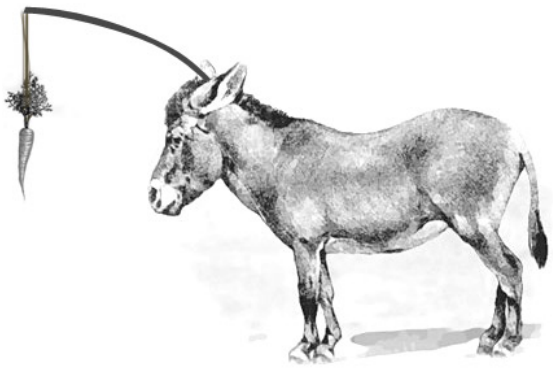

Figure 2.1: Reference dependent on the manipulated variable

The problem is that according to Eq. (2.22) the $T_{wo.SP}$ depends on the mass flow $\dot{m}$, which will be the manipulated variable. The control law is then implicit and unstable. The higher $T_{wo.SP}$ is given as a reference, the higher $\dot{m}$ is provided and therefore the higher $T_{wo.SP}$ is again demanded. It reminds the situation of a donkey carrying a carrot hanging before it (Fig. 2.1). The reference (position of the carrot) moves in the same direction and of the same value as the manipulated variable (donkey position).

Another way of $T_{wo.SP}$ reference computation has to be used and we again turn to the steady state. From the steady state temperature profile, Eq. (2.10) and Eq. (2.11) we get

$$\Theta(x) = \frac{T_{wo} - T_{ai}}{T_{wi} - T_{ai}} = e^{-\frac{UA}{\dot{m}c_p}x}. \tag{2.23}$$

Part of Eq. (2.21) can be rewritten as

$$\begin{aligned}(T_{wi} - T_{wo}) &= T_{wi} - T_{ai} - T_{wo} + T_{ai} = T_{wi} - T_{ai} - \frac{T_{wo} - T_{ai}}{T_{wi} - T_{ai}}\,(T_{wi} - T_{ai}) \\ &= T_{wi} - T_{ai} - \Theta_{out}\,(T_{wi} - T_{ai}) = (T_{wi} - T_{ai})\,(1 - \Theta_{out})\end{aligned} \tag{2.24}$$

and we get the relation

$$Q = \dot{m}c_p\,(T_{wi} - T_{ai})\,(1 - \Theta_{out})\,. \tag{2.25}$$

Let's focus only on the point where the water leaves the heat exchanger, i.e. the point $x = 1$. From Eq. (2.23) it is possible to express

$$\dot{m}(t) = -\frac{UA}{c_p ln(\Theta_{out}(t))}\ . \tag{2.26}$$

Then we substitute $\dot{m}(t)$ in Eq. (2.21) by Eq. (2.26) and get

$$Q = -\frac{UA}{c_p ln(\Theta_{out})} c_p\,(T_{wi} - T_{wo})\,. \tag{2.27}$$

The Eq. (2.27) is then transformed into

$$Q = -\frac{UA}{ln(\Theta_{out})}\,(T_{wi} - T_{ai})\,(1 - \Theta_{out})\,. \tag{2.28}$$

This equation has an analytical solution for Θ_{out} which is

$$\Theta_{out} = -\frac{Q}{UA\,(T_{wi} - T_{ai})} W\left(-\frac{UA\,(T_{wi} - T_{ai})}{Q} e^{-\frac{UA(T_{wi}-T_{ai})}{Q}}\right), \tag{2.29}$$

where $W(.)$ is the Lambert W function.

From the value of Θ_{out} it is possible to get the output water temperature set-point $T_{wo.SP}$ as

$$T_{wo.SP} = \Theta_{out}\,(T_{wi} - T_{ai}) + T_{ai} = T_{ai} + f(Q_{SP}) W\left(f(Q_{SP}) e^{f(Q_{SP})}\right). \tag{2.30}$$

Mass-flow-dependent UA

In the previous subsection an explicit formula for T_{wo} was found, because we assumed the heat transfer coefficient UA to be constant for all values of the mass flow $\dot{m}$. However, in the real heat exchanger, the heat transfer coefficient consists of the heat transfer coefficient from water to body UA_{WB} and from the heat exchanger body to air UA_{BA}. Moreover, the value of UA_{WB} differs for different $\dot{m}$. The combination of UA_{WB} with UA_{BA} to UA is

$$UA = \left(UA_{WB}^{-1} + UA_{BA}^{-1}\right)^{-1}. \tag{2.31}$$

If we take into account the UA to be exponentially mass-flow-dependent,

$$UA_{WB}(\dot{m}) = a\dot{m}^b, \tag{2.32}$$

the Eq. (2.23) changes into

$$\Theta_{out} = e^{-\frac{1}{\left(\frac{1}{UA_{WB}} + \frac{1}{UA_{BA}}\right)\dot{m}c_p}} = e^{-\frac{1}{\left(\frac{\dot{m}^{-b}}{a} + \frac{1}{UA_{BA}}\right)\dot{m}c_p}}. \tag{2.33}$$

The equation to be solved is obtained by substitution of Θ_{out} from Eq. (2.33) to Eq. (2.25)

$$Q = \dot{m}c_p\,(T_{wi} - T_{ai}) - \dot{m}c_p\,(T_{wi} - T_{ai})\, e^{-\frac{1}{\left(\frac{\dot{m}^{1-b}}{a} + \frac{\dot{m}}{UA_{BA}}\right)c_p}}. \tag{2.34}$$

There is no analytical solution of Eq. (2.34) for $\dot{m}$, but it can be solved numerically. When the $\dot{m}^{SP}$ is obtained, Θ_{out}^{SP} is computed according to Eq. (2.33) and from Θ_{out}^{SP} the value of $T_{wo.SP}$ can be calculated by Eq. (2.30).

2.2.4 Heat flow estimation

The object of this thesis is the heat flow Q [W] control of a heat exchanger. But it is definitely not easy to measure the heat flow; Although the steady state value can be

computed from the temperature difference of the inlet and outlet water, as stated in Eq. (2.21). An advantage of this approach is, that we do not need to know the value of the heat exchanger heat transfer coefficient UA. However, this heat flow estimate doesn't reflect the real heat flow during transients, so it is absolutely unsuitable for control.

Another way of a heat flow estimation is an estimate according to Eq. (2.35)

$$Q = UA \cdot LMTD, \tag{2.35}$$

where $LMTD$ (explained in [12]) is the *Logarithmic Mean Temperature Difference*

$$LMTD = \frac{\Delta T|_{x=0} - \Delta T|_{x=1}}{\ln\left(\frac{\Delta T|_{x=0}}{\Delta T|_{x=1}}\right)} = \frac{(T_{wi} - T_{ai}) - (T_{wo} - T_{ai})}{\ln\left(\frac{T_{wi}-T_{ai}}{T_{wo}-T_{ai}}\right)}. \tag{2.36}$$

Let's define an *Unused water heat content* Θ as

$$\Theta = \frac{T_{wo} - T_{ai}}{T_{wi} - T_{ai}}, \tag{2.37}$$

which is a number in range [0–1] and it is $1 - \rho$, where ρ is a ratio of the heat, the water did deliver to the heat exchanger, to the heat it could deliver, if it stood long enough to cool down to the temperature of surrounding air. It allows us to rewrite Eq. (2.36) as

$$LMTD = \frac{\Theta - 1}{\ln(\Theta)} (T_{wi} - T_{ai}) \tag{2.38}$$

and Eq. (2.35) becomes

$$Q = UA \frac{\Theta - 1}{\ln(\Theta)} (T_{wi} - T_{ai}) \ . \tag{2.39}$$

2.2.5 Relative heat flow concept

The above explained methods of heat estimation both have some limits; Either it can be used only for steady state or it is required to know the value of UA. Hence we tried to estimate and control a relative heat

$$Q_r = \frac{Q}{Q_{max}}. \tag{2.40}$$

The key step is to somehow estimate the relative heat. We can use the Eq. (2.39) and substitute it into Eq. (2.40), which gives

$$Q_r = \frac{(\Theta - 1)}{\ln(\Theta)} \frac{\ln(\Theta_{max})}{(\Theta_{max} - 1)} \frac{UA(\dot{m})}{UA_{max}}. \tag{2.41}$$

Assume, that we do not know the dependency of UA on the mass flow $\dot{m}$. Let's compensate the lack of information by a correction factor c, so that the relative heat flow will be defined as

$$Q_r = \left(\frac{(\Theta - 1)}{\ln(\Theta)} \frac{(\Theta_{max} - 1)}{\ln(\Theta_{max})} \right)^c. \tag{2.42}$$

2.3 Heat exchanger simulation model

For dynamic simulations a simulation model was developed by advective *Finite Volume Method* (FVM) according to work of Dostál and Havlena [7]. The number of states of a system with distributed parameters is infinity, therefore it is not possible to model it by a set of state-space equations. One possible way is to split the system into smaller segments and to model these segments as a lumped element model.

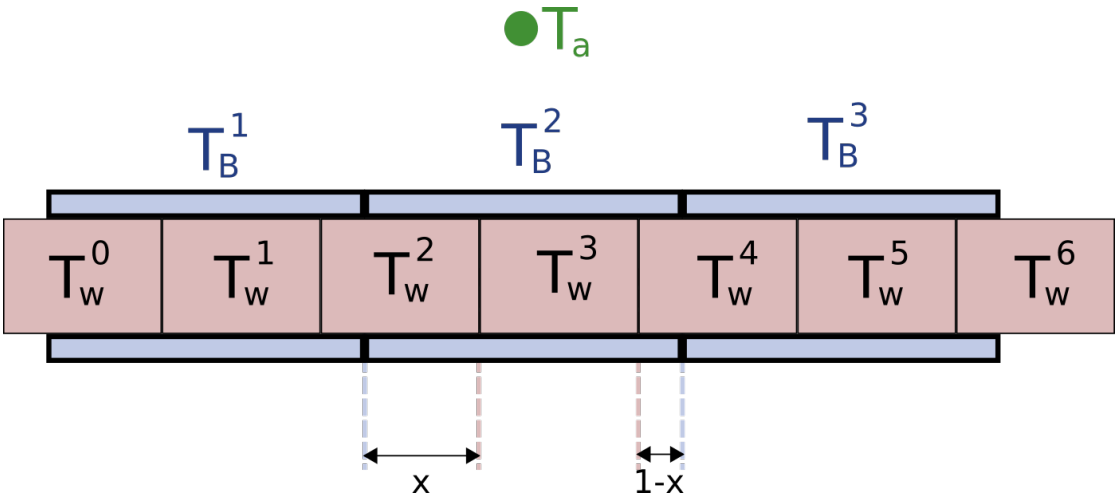

Figure 2.2: Illustration of a segment model of HX

To simulate a behavior of a heat exchanger a hybrid model combining a continuous and a discrete part was developed. Both the water in the HX and the tube are divided into several segments. The continuous step of the simulation starts with a tube completely filled with water segments and one (zero-th) segment is right before the beginning of the tube. During the continuous simulation step, the water segments are moved, till the last water segment leaves completely the tube. Then, the discrete step is proceeded; Each water segment is moved back to the starting position, but its current temperature value is assigned to the next water segment (the one with a higher index), and its actual value gets taken from the previous segment.

The model of the HX tube is divided into M segments and the water flowing through the tube is divided into N segments. The situation is depicted in Fig. 2.2. The ratio of M, N holds $N_{wb} = \frac{N-1}{M} \in \mathcal{N}$, so there is exactly one water segment left after a complete filling of the tube.

A state space model of the heat exchanger is

$$\begin{bmatrix} \dot{T}_w \\ \dot{T}_b \end{bmatrix} = \mathbf{A} \begin{bmatrix} T_w \\ T_b \end{bmatrix} + \mathbf{B}\, T_{ai}. \tag{2.43}$$

Let's neglect the heat conduction between the neighboring liquid segments. The state equations representing the temperature of an l-th water segment are

$$\begin{aligned} \frac{C_w}{N}\dot{T}_w^l &= -Q_{1-x}^l - Q_x^l \ , \text{ for } l = k\,N_{wb},\ k = 1, 2, 3, \ldots \\ \frac{C_w}{N}\dot{T}_w^l &= -Q^l, \text{ otherwise,} \end{aligned} \tag{2.44}$$

where x [0–1] is a relative distance the water traveled since the last discrete step, C_w [$\mathrm{J\,K^{-1}}$] a heat capacity of the water in the HX, Q_x^l [W] is a heat flow between the l-th water segment and the k-th tube segment, Q_{1-x}^l [W] is a heat flow between the l-th water segment and the $(k+1)$-th tube segment and Q^l [W] is a heat flow between the l-th water segment and k-th tube segment in a situation that the whole l-th water segment is in one tube segment.

Let's neglect the heat transfer between the neighboring body segments. The state equations of a k-th body segment temperature is

$$\frac{C_b}{M}\dot{T}_b^k = Q_x^l + \sum_{i=l+1}^{l+N_{lb}-1} Q^i + Q_{1-x}^l - Q_{ab}^k \ , \text{ for } l = k\,N_{wb},\ k = 1, 2, 3, \ldots \tag{2.45}$$

where Q_{ab} is a heat flow between the tube body segment and the air and C_b [$\mathrm{J\,K^{-1}}$] is a heat capacity of the HX tube. The heat flows between the water and the tube, which are used in Eq. (2.44) and Eq. (2.45), are computed as follows

$$Q_{1-x}^l = (1-x)\frac{UA_{wb}}{N}\left(T_w^l - T_b^k\right) \tag{2.46}$$

$$Q_x^l = x\frac{UA_{wb}}{N}\left(T_w^l - T_b^k\right) \tag{2.47}$$

$$Q^i = \frac{UA_{wb}}{N}\left(T_w^i - T_b^k\right) \tag{2.48}$$

$$Q_{ab}^k = \frac{UA_{ab}}{M}\left(T_{ai}^k - T_b^k\right) \ , \tag{2.49}$$

where UA_{wb}[$\mathrm{W\,K^{-1}}$] is the heat transfer coefficient between the water and the tube and UA_{wb}[$\mathrm{W\,K^{-1}}$] the heat transfer coefficient between the tube and the surrounding air.

Then we can rewrite the equations (2.44) as

$$\begin{aligned}
\dot{T}_w^0 &= -x\frac{UA_{wb}}{C_w}\left(T_w^{1+N_{lb}} - T_b^1\right) && (2.50)\\
\dot{T}_w^1 &= -\frac{UA_{wb}}{C_w}\left(T_w^1 - T_b^1\right) && (2.51)\\
\dot{T}_w^2 &= -\frac{UA_{wb}}{C_w}\left(T_w^2 - T_b^1\right) && (2.52)\\
&\vdots \quad \vdots \quad \vdots \\
\dot{T}_w^{1+N_{lb}-1} &= -\frac{UA_{wb}}{C_w}\left(T_w^{1+N_{lb}-1} - T_b^1\right) && (2.53)\\
\dot{T}_w^{1+N_{lb}} &= -\frac{UA_{wb}}{C_w}\left[(1-x)\left(T_w^{1+N_{lb}} - T_b^1\right) + x\left(T_w^{1+N_{lb}} - T_b^2\right)\right] && (2.54)\\
\dot{T}_w^{1+N_{lb}+1} &= -\frac{UA_{wb}}{C_w}\left(T_w^{1+N_{lb}+1} - T_b^2\right) && (2.55)\\
&\vdots \quad \vdots \quad \vdots
\end{aligned}$$

and the set of the body elements temperature state equations (2.45) as

$$\begin{aligned}
\dot{T}_b^1 &= x\frac{M}{N}\frac{UA_{wb}}{C_b}\left(T_w^0 - T_b^1\right) && (2.56)\\
&+ \frac{M}{N}\frac{UA_{wb}}{C_b}\left(T_w^1 - T_b^1 + T_w^2 - T_b^1 + \ldots + T_w^{N_{lb}-1} - T_b^1\right)\\
&+ (1-x)\frac{M}{N}\frac{UA_{wb}}{C_b}\left(T_w^{N_{lb}} - T_b^1\right)\\
\dot{T}_b^2 &= x\frac{M}{N}\frac{UA_{wb}}{C_b}\left(T_w^{N_{lb}} - T_b^2\right)\\
&+ \frac{M}{N}\frac{UA_{wb}}{C_b}\left(T_w^{N_{lb}+1} - T_b^2 + T_w^{N_{lb}+2} - T_b^2 + \ldots + T_w^{2N_{lb}-1} - T_b^2\right)\\
&+ (1-x)\frac{M}{N}\frac{UA_{wb}}{C_b}\left(T_w^{2N_{lb}} - T_b^2\right)\\
\vdots &\quad \vdots \quad \vdots
\end{aligned}$$

These state equations rewritten into a matrix form consist of state matrices that are built as follows: the $\mathbf{A}$ matrix consists of four submatrices

$$\mathbf{A} = \begin{bmatrix} \mathbf{A}_{ww} & \mathbf{A}_{wb} \\ \mathbf{A}_{bw} & \mathbf{A}_{bb} \end{bmatrix}. \qquad (2.57)$$

$\mathbf{A}_{ww}$ is a state matrix of influence of water segments temperature on water segments temperature derivative. $\mathbf{A}_{wb}$ describes the influence of body element temperatures on the derivatives of water segments temperatures and it is similar by $\mathbf{A}_{bw}$ and $\mathbf{A}_{bb}$. These

submatrices are

$$\mathbf{A}_{ww} = \begin{array}{c} \\ \dot{T}_w^0 \\ \dot{T}_w^1 \\ \vdots \\ \dot{T}_w^N \end{array} \begin{array}{c} \begin{array}{cccc} T_w^0 & T_w^1 & \dots & T_w^N \end{array} \\ \begin{bmatrix} -1 & & & \\ & -1 & & \\ & & \ddots & \\ & & & -1 \end{bmatrix} \end{array} \beta_W \ ,$$

$$\mathbf{A}_{wb} = \begin{array}{c} \\ T_w^0 \\ T_w^1 \\ T_w^2 \\ \vdots \\ T_w^{N_{wb}-1} \\ T_w^{N_{wb}} \\ T_w^{N_{wb}+1} \\ T_w^{N_{wb}+2} \\ \vdots \\ T_w^{N-N_{wb}} \\ T_w^{N-N_{wb}+1} \\ T_w^{N-N_{wb}+2} \\ \vdots \\ T_w^{N-1} \end{array} \begin{array}{c} \begin{array}{cccccc} T_b^1 & T_b^2 & \dots & T_b^M \end{array} \\ \begin{bmatrix} x & & & \\ 1 & & & \\ 1 & & & \\ \vdots & & & \\ 1 & & & \\ (1-x) & x & & \\ & 1 & & \\ & 1 & & \\ & & \ddots & \\ & & & x \\ & & & 1 \\ & & & 1 \\ & & & \vdots \\ & & & (1-x) \end{bmatrix} \end{array} \beta_W,$$

$$\mathbf{A}_{bw} = \begin{array}{c} \\ T_b^1 \\ T_b^2 \\ \vdots \\ T_b^M \end{array} \begin{array}{c} \begin{array}{ccccccccc} T_w^{N_{wb}} & \dots & T_w^{2N_{wb}} & \dots & T_w^{N-N_{wb}-1} & \dots & T_w^{N-1} \end{array} \\ \begin{bmatrix} \mathbf{I}_r & (1-x) & & & & & \\ x & & \mathbf{I}_r & (1-x) & & & \\ & & & \ddots & & & \\ & & & & x & \mathbf{I}_r & (1-x) \end{bmatrix} \end{array} \beta_B$$

where $\mathbf{I}_r = [1 \dots 1]$.

$$\mathbf{A}_{bb} = \begin{array}{c} \\ T_b^1 \\ \vdots \\ T_b^M \end{array} \begin{array}{c} \begin{array}{ccc} T_b^1 & \dots & T_b^M \end{array} \\ \begin{bmatrix} -1 & & \\ & \ddots & \\ & & -1 \end{bmatrix} \end{array} (N_{wb}\beta_B + \beta_A) \ ,$$

where the coefficients $\beta_W, \beta_B, \beta_A$ are

$$\begin{aligned} \beta_W &= \frac{UA_{wb}}{C_w} \\ \beta_B &= N_{wb}\frac{UA_{wb}}{C_b} \\ \beta_A &= \frac{UA_{ba}}{C_b} \ . \end{aligned} \tag{2.58}$$

A matrix of the system inputs is

$$\mathbf{B} = \begin{matrix} \\ T_w^0 \\ \vdots \\ T_w^{N-1} \\ T_b^1 \\ \vdots \\ T_b^M \end{matrix} \begin{matrix} T_{ai} \\ \left[\begin{matrix} 0 \\ \vdots \\ 0 \\ 1 \\ \vdots \\ 1 \end{matrix}\right. \end{matrix} \beta_A \ . \tag{2.59}$$

2.3.1 Heat exchanger discretization

Now we have a hybrid model of the HX. It would be nice to discretize the continuous part of the model to obtain a pure discrete system. If the system is linear and time-invariant then it is a simple process to obtain the discrete state-space matrices. These matrices are

$$\begin{aligned} \mathbf{A}_d &= \mathbf{\Phi}(t_0, T) \\ \mathbf{B}_d &= \left(\int_{\tau=0}^{T} \mathbf{\Phi}(t_0, \tau) d\tau \right) \mathbf{B} \\ \mathbf{C}_d &= \mathbf{C} \\ \mathbf{D}_d &= \mathbf{D} \ , \end{aligned} \tag{2.60}$$

where $\mathbf{\Phi}(t_0, T)$ is the state transition matrices between the state during the sampling time (t_0, T). In the LTE case the state transition matrix is a matrix exponential $\boldsymbol{\phi}(t_0, T) = e^{\mathbf{A}T}$. Since our system is a time-varying one this simple computation method cannot be used.

Forward Euler method

Such a continuous state space model can be discretized by a forward Euler method. This method is described in detail in [7]. Two assumptions must hold

- All heat exchanger inputs are constant in between sampling instances.
- Water elements exchange heat with HX body as if the elements not moved during a sampling interval.

The time derivative can then be approximated by an explicit Euler method

$$\frac{\mathrm{d}x}{\mathrm{d}t} = \frac{x(k+1) - x(k)}{\tau_s}, \tag{2.61}$$

where τ_s is the sampling interval.

State transition matrix

The state-space matrices are time-varying though, but it is possible to nicely separate the time-invariant and the time-varying part such that

$$\begin{aligned} \mathbf{A} &= \mathbf{A}_1 + \mathbf{A}_2 t \\ \mathbf{B} &= \mathbf{B}_1 + \mathbf{B}_2 t \ . \end{aligned}$$

The system is then

$$\dot{\mathbf{x}}(t) = (\mathbf{A}_1 + \mathbf{A}_2 t)\, \mathbf{x}(t) + (\mathbf{B}_1 + \mathbf{B}_2 t)\, u(t) \ . \tag{2.62}$$

The key step is to find a state transition matrix $\Phi(t, t_0)$, so that

$$\mathbf{x}(t) = \mathbf{\Phi}(t, t_0)\mathbf{x}(t_0) + \int_{t_0}^{t} \phi(t, \tau)\mathbf{B}(\tau)\mathbf{u}(\tau)d\tau \ . \tag{2.63}$$

If the system was a first-order then it would be possible to solve the differential equation analytically and get $\mathbf{\Phi}(t_0, T)$. However, this naive approach can't be used with a higher-order case.

Although there are several ways how to find the state transition matrices, they are usually restricted to some special cases of the time-varying systems. Let's take a look if some of them could be used for our system.

Analytical solution - PBS

The analytical solution of such a system could be expressed by a Peano-Baker's serie (PBS) [13]

$$\mathbf{\Phi}(t; t_0) = \mathbb{1} + \int_{t_0}^{t} \boldsymbol{A}(\tau)d\tau + \int_{t_0}^{t} \boldsymbol{A}(\tau_1) \int_{t_0}^{\tau_1} \boldsymbol{A}(\tau_2)d\tau_2 d\tau_1 + \ldots = \mathbb{1} + \sum_{n=1}^{\infty} \mathcal{I}_n, \tag{2.64}$$

where

$$\mathcal{I}_n(t) = \int_{t_0}^{t} \boldsymbol{A}(\tau_1) \int_{t_0}^{\tau_1} \boldsymbol{A}(\tau_2) \dots \int_{t_0}^{\tau_{n-1}} \boldsymbol{A}(\tau_n) d\tau_n \dots d\tau_2 d\tau_1 \ . \tag{2.65}$$

Even that it is an infinite serie and therefore it is not very useful for computational purposes, for some special cases of $\mathbf{A}(t)$ it is possible to find a finite analytical solution. If the state matrix $\mathbf{A}(t)$ commutates for all t, then the state transition matrix is

$$\mathbf{\Phi}(t, t_0) = exp\left[\int_{t_0}^{t} \mathbf{A}(\tau) d\tau\right] \ . \tag{2.66}$$

If the $\mathbf{A}(t)$ matrix holds any of the following conditions ([10]) then both $\mathbf{A}(t)$ and $\int_{t_0}^{t} \mathbf{A}(\tau) d\tau$ commute for all t:

1. $\mathbf{A}(t)$ is constant
2. $\mathbf{A}(t) = \alpha(t)\mathbf{M}$ where $\alpha(t)$ is a scalar function and $\mathbf{M} \in \mathcal{R}^{nxn}$ is a constant matrix
3. $\mathbf{A}(t) = \sum_i \alpha_i(t)\mathbf{M}_i$ where $\alpha_i(t)$ are scalar functions and $\{\mathbf{M}_i\}$ is a set of matrices that commute: $\mathbf{M}_i\mathbf{M}_j = \mathbf{M}_j\mathbf{M}_i$
4. $\mathbf{A}(t)$ has a time-invariant basis of eigenvectors spanning $\mathcal{R}^n$.

Since the heat exchanger state matrix unfortunately doesn't fulfill any of the mentioned conditions, there is no easily reachable analytical solution of $\mathbf{A}_d$.

Numerical solution

It is not possible to find the state transition matrix analytically, but a trick mentioned in [3] leads to a numerical solution. The way is to numerically simulate the initial state response for several initial conditions

$$x^1(t_0) = \begin{bmatrix} 1 \\ 0 \\ 0 \\ \vdots \\ 0 \end{bmatrix}, \ x^2(t_0) = \begin{bmatrix} 0 \\ 1 \\ 0 \\ \vdots \\ 0 \end{bmatrix}, \ \dots, \ x^n(t_0) = \begin{bmatrix} 0 \\ 0 \\ 0 \\ \vdots \\ 1 \end{bmatrix}, \tag{2.67}$$

which gives the responses $x^1(t), x^2(t), \dots, x^n(t)$ and the state transition matrix is then

$$\mathbf{\Phi}(t, t_0) = \left[x^1(t) \dots x^n(t)\right] \ . \tag{2.68}$$

The advantage of this method is that we get an exact discretized model which is sufficient unless there is no need to change the sampling period. However if there is such

a need then the state transition matrix has to be re-computed for every sampling period change. The computation of the state transition matrix is time consuming because the system has to be simulated n-times to get one $\mathbf{\Phi}(t, t_0)$. In our hybrid model the sampling period is spatially constant but it changes with the mass flow. For every mass flow change the system matrices have to be recomputed which is not really efficient. However, we are going to continue the research and try to find a way, how to accomplish an exact discretization of the heat exchanger in an elegant way.

Chapter 3

Control

In this chapter, the control algorithms are introduced. The variables being controlled were the outlet water temperature T_{wo} [°C], heat flow Q [W] and relative heat flow Q_r [0–1]. Two controllers were tested; The controller introduced by Shang [15], which is based on control of the heat exchanger temperature profile, and controller introduced by Sandoval [8], which is a robust controller suitable for transport-delay systems. Three approaches of heat flow control are outlined in this chapter. The first one is to recompute the Q reference value to $T_{wo.SP}$ value and then control T_{wo}, which is an open loop control without a feedback from Q. Another option is to estimate the value of Q as explained in the previous chapter and to use this estimate for control. Third way is to control the relative heat flow. A more accurate version of the second option is implementation of an observer of the heat transfer coefficient UA.

3.1 Boiler control

For our experiments, it is useful to have a possibly constant temperature of the HX inlet water. For this purpose, a boiler controller (Fig. 3.1) was implemented. It contains a feedback from the boiler outlet water temperature T_{bo} and also an estimate of the current heat flow in the heat exchanger as feed-forward. The boiler control action is

$$P_{boiler} = PI(e, l_{low}, l_{up}) + Q_{tube\,loss} + Q_{HX}, \tag{3.1}$$

where $e = T_{bo.SP} - T_{bo}$ is the control error, $PI(e, l_{low}, l_{up})$ is an output of a PI controller

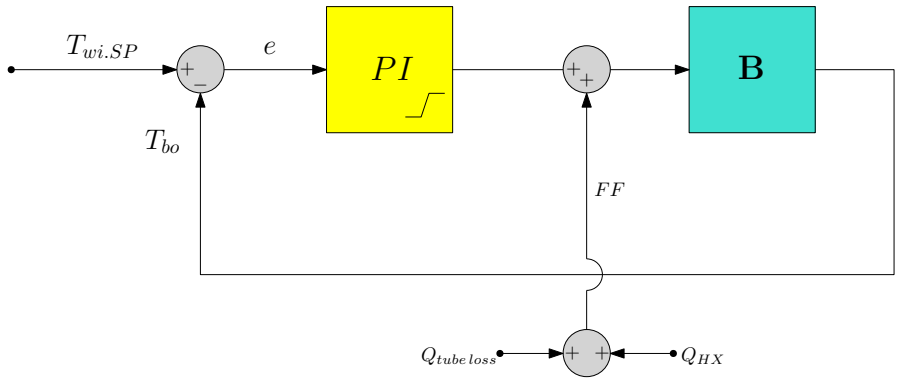

Figure 3.1: Boiler control scheme

with floating output limits l_{low}, l_{up}. P_{max} $[W]$ is the maximal boiler power obtained from the boiler characteristics (Fig. 4.6). The feed-forward component is

$$FF = Q_{tube\,loss} + Q_{HX}, \tag{3.2}$$

where, $Q_{tube\,loss}$ $[W]$ is the heat flow from the non-HX tubes to air and Q_{HX} $[W]$ is the current heat exchanger heat flow. Their values are obtained from

$$Q_{tube\,loss} = UA_{tubes}\, LMTD \tag{3.3}$$
$$Q_{HX} = \dot{m} c_p \left(T_{wi} - T_{wo}\right), \tag{3.4}$$

where $LMTD$ is the Logarithmic Mean Temperature Difference. Bounds limiting the output of the PI controller are defined as

$$l_{low} = -FF \tag{3.5}$$
$$l_{up} = 1 - FF. \tag{3.6}$$

This restriction ensures, that the output of the boiler controller gives a value from range [0–1].

A value of UA_{tubes} was found by an experiment; No water was pumped to the heat exchanger and the T_{bo} value was held on a constant value. When it reached the steady state, we measured the boiler power by an external watt-meter and computed UA_{tubes} according to Eq. (2.5). However, this identification experiment neglected the heat transfer rate of tubes between the double-T segment (explained in the Testbed chapter) and the heat exchanger, which is a big piece of brass with a significant thermal conductivity. Finally, we estimated the $Q_{tube\,loss}$ from difference between the mean power of boiler and estimated mean heat flow of the heat exchanger.

3.2 Shang T_{wo} controller

This section describes a controller that controls the temperature of water leaving the heat exchanger. By design, the controller is using the information of a spatial temperature profile of the heat exchanger. A similar controller was described by Shang in [15] and references a temperature profile controller previously introduced by Hanczyc and Palazoglu in [9].

3.2.1 General controller derivation

The heat exchanger could be characterized by a PDE (introduced in 2.1). With a help of Method of Characteristics [11], it is possible to reduce the PDE into a set of ODEs. This method utilizes the characteristic curves along which the PDE turns into an ODE.

Let's have a quasi linear PDE

$$\begin{aligned} &\frac{\partial v}{\partial t} + a(v,x,u)\frac{\partial v}{\partial x} = f(v) + g(v)u, \\ &v|_{x_b} = v_b, \\ &y = h(v)|_{x_e} \end{aligned} \tag{3.7}$$

where x is a spatial position within the HX, $v \in \mathcal{H}\left[(0,L),R\right]$ is a distributed state variable, t is time, $u \in R$ the manipulated variable, $a(v,x,u)$, $f(v)$ and $g(v)$ are continuous functions, x_b and x_e are points where fluid enters and exits the HX respectively.

Such a quasi-linear PDE can be reduced into an ODE system in (t,x,v) coordinates. The characteristic curves $t(s), x(s), v(s)$ are obtained by solving the following system of ODEs:

$$\begin{aligned} \frac{\partial t}{\partial s} &= 1, \\ \frac{\partial x}{\partial s} &= a(v,x,u), \\ \frac{\partial v}{\partial s} &= f(v) + g(v)u\ . \end{aligned} \tag{3.8}$$

The vector field describing the variation of (t,x,v) along the characteristics curves is

$$\xi = [1\ , a(v,x,u),\ \ f(v) + g(v)u]\ . \tag{3.9}$$

It is obvious, that if the system (3.8) is supposed to be controllable, both $\frac{\partial a(v,x,u)}{\partial u}$ and $g(v)$ cannot be zero. Let's assume that the system output (value of $h(v)$ at point x_e) reaches

the desired reference value r; This could be interpreted so, that along the characteristic curves the output $h(v)$ reaches its set-point value, while the coordinate x reaches x_e. Let's define $v_{in} = v(x)|_{x_{in}}$, then the following is true

$$r - h(v_{in}) = \int_{x_{in}}^{x_e} \frac{L_\xi h(v)}{a(v,x,u)} dx \ . \tag{3.10}$$

The Lie derivative of function $h(v)$ along the vector field ξ is

$$L_\xi h(v) = \frac{\partial h(v)}{\partial t} \cdot 1 + \frac{\partial h(v)}{\partial x} \cdot a(v,x,u) + \frac{\partial h(v)}{\partial v} \left(f(v) + g(v)u\right) = f(v) + g(v)u \ . \tag{3.11}$$

Assume a special case $a(v,x,u) = a'(v,x)u$, then Eq. (3.10) can be rewritten as

$$r - h(v_{in}) = \int_{x_{in}}^{x_o} \frac{f(v) + g(v)u}{a'(v,x)u} dx = \int_{x_{in}}^{x_o} \frac{f(v)}{a'(v,x)u} dx + \int_{x_{in}}^{x_o} \frac{g(v)}{a'(v,x)} dx \ . \tag{3.12}$$

Then we can extract the manipulated variable and form a control law

$$u = \frac{\int_{x_{in}}^{x_o} \frac{f(v)}{a'(v,x)} dx}{r - h(v_{in}) - \int_{x_{in}}^{x_o} \frac{g(v)}{a'(v,x)} dx} \ . \tag{3.13}$$

3.2.2 HX controller implementation

Now we use the general steps proposed in the previous section and apply them to the heat exchanger model. This controller was introduced in paper by Shang [15] and compared with the Hanczyc and Palazoglu controllers. It uses the knowledge of the mean spatial profile temperature $\langle T \rangle$ to control T_{wo}. The manipulated variable is the mass flow rate $\dot{m}$ [kg h^{-1}].

Let's consider x to take a value among $x \in [0,1]$. The simulated heat exchanger is described by a PDE

$$\begin{aligned} &\frac{\partial T(x,t)}{\partial t} c_p A \rho_w + \dot{m}(t) c_p \frac{\partial T(x,t)}{\partial x} + UA\left(T(x,t) - T_A\right) = 0 \\ &T(0,t) = T_{wi}(t), \\ &T_{wo}(t) = T(1,t), \end{aligned} \tag{3.14}$$

where $T(x,t)$ is a temperature of the fluid in the heat exchanger and T_{ai} is a temperature of the surrounding air, U [$^W/_{m^2K}$] the overall heat transfer coefficient, A an area of the heat exchanger surface and c_p [$^J/_{kgK}$] the fluid specific heat capacity at constant pressure. The vector field for this PDE of Eq. (3.14) is

$$\xi = [c_p A \rho_w, \ \dot{m} c_p, \ -UA(T - T_A)] \ .$$

Using the method of characteristics described above, we get a condition for the manipulated variable

$$T_{wo.SP} - T_{wi} = \int_0^1 \frac{L_\xi T}{\dot{m}c_p} dx = \int_0^1 \frac{UA(T_A - T)}{\dot{m}c_p} = \frac{UA}{\dot{m}c_p} \left(T_A - \overbrace{\int_0^1 T dx}^{\langle T \rangle} \right), \tag{3.15}$$

which can be transformed into an equation

$$\frac{UA}{\dot{m}c_p} = \frac{T_{wo.SP} - T_{wo}}{T_A - \langle T \rangle}, \tag{3.16}$$

where $\langle T \rangle$ denotes the mean value of the spatial temperature profile in the heat exchanger and $T_{wo.SP}$ the set-point value for T_{wo}. The estimation of $\langle T \rangle$ is explained in section 2.2.

This approach requires knowledge of the heat transfer coefficient UA [$\mathrm{W\,K^{-1}}$], which is mainly composed of the heat transfer coefficient between water and the tube $UA_{WB}(\dot{m})$ and the heat transfer coefficient between the tube and the surrounding air UA_{BA}. The resulting value of UA is

$$UA = \left(\frac{1}{UA_{WB}(\dot{m})} + \frac{1}{UA_{BA}} \right)^{-1}. \tag{3.17}$$

However, the value of UA_{WB} depends on the water mass flow (which is the manipulated variable) by

$$UA_{WB} = a\dot{m}^b \ . \tag{3.18}$$

Therefore Eq. (3.16) is rewritten as

$$\frac{\dot{m}c_p}{UA(\dot{m})} = \frac{T_A - \langle T \rangle}{T_{SP} - T_{wo}} \tag{3.19}$$

$$\dot{m}c_p \left(UA_{BA}^{-1} + \frac{1}{a}\dot{m}^{-b} \right) = \frac{T_A - \langle T \rangle}{T_{SP} - T_{wo}} \tag{3.20}$$

so the manipulated variable $\dot{m}$ is obtained as a solution of the implicit equation

$$\frac{1}{UA_{BA}}\dot{m} + \frac{1}{a}\dot{m}^{1-b} - \frac{T_A - \langle T \rangle}{T_{SP} - T_{wo}} = 0 \ . \tag{3.21}$$

For the sake of preventing a division by zero in the case, when $T_{wo.SP} = T_{wo}$, we transform Eq. (3.21) to the form

$$\frac{T_{wo.SP} - T_{wo}}{UA_{BA}}\dot{m} + \frac{T_{wo.SP} - T_{wo}}{a}\dot{m}^{1-b} - (T_A - \langle T \rangle) = 0 \ . \tag{3.22}$$

Since the parameters a, b can change for different materials, it is not possible to find a universal analytical solution Eq. (3.22). Therefore it has to be solved numerically by the Simulink solver during the simulation.

Integral part

Although the Shang controller computes the mean value of the whole temperature profile, it is still something like a special form of a P controller. Since it has no integral part, there will be steady state offset due to model mismatch. An improvement can be achieved by adding an integral part, as introduced in [15]. The control law Eq. (3.15) changes into

$$T_{wo.SP} - T_{wi} = \frac{UA}{\dot{m}c_p}\left(T_A - \int_0^1 T dx\right) + \lambda \int_0^t \left(T_{wo} - T_{wo.SP}\right) d\tau, \tag{3.23}$$

where λ is a tuning parameter. The Eq. (3.22) then gets a form

$$\begin{aligned}&\left(T_{wo.SP} - T_{wi} - \lambda \int_0^t \left(T_{wo} - T_{wo.SP}\right) d\tau\right) \frac{\dot{m}}{UA_{BA}} \\ &+ \frac{T_{wo.SP} - T_{wi}}{a} \dot{m}^{1-b} - \left(T_A - \langle T \rangle\right) = 0.\end{aligned} \tag{3.24}$$

The mass flow $\dot{m}$ that fulfills the Eq. (3.24) is supposed to control the output water temperature T_{wo} without a steady-state offset.

3.3 Shang Q controller

The aim of the heat exchanger is to transfer heat to the surrounding area. Therefore our next aim is to control the heat flow Q [W], nevertheless there is a problem with the heat flow measurement. Although it is possible to estimate the heat flow according to Eq. (2.21), we do not have a mechanism to use the Q estimate as an input to the Shang controller. Hence if we consider our knowledge of UA to be accurate enough, we can implement an open-loop controller. We simply compute the outlet water temperature set-point $T_{wo.SP}$ from the heat flow reference Q_{SP}, as stated in section 3.2, and the controller again controls T_{wo}.

3.4 Sandoval T_{wo} controller

This controller is described in detail by Sandoval in [8]. He addressed a framework for synthesis of robust controllers for a FOPDE system with varying input transport-delay.

3.4.1 Control problem

Same as in the case of Shang controller in the previous section 3.2, the FOPDE description of the heat exchanger Eq. (3.7) was used. The system of three ODEs obtained by Method of Characteristics Eq. (3.8) can be under assumption $t = s$ simply reduced to

$$\frac{\partial x}{\partial t} = a(v, x, u(t)),\ x(t_0) = x_0 \tag{3.25}$$

$$\frac{\partial v}{\partial t} = f(v),\ v(t_0) = v_0 \tag{3.26}$$

from that we get

$$x = x_0 + w(t) - w(t_0), \tag{3.27}$$

$$v(t, t_0) = \phi^f_{t-t_0}(v_0), \tag{3.28}$$

where $w(t) = \int_0^t a(v, x, u(\lambda))d\lambda$ denotes the amount of fluid that has already passed through the heat exchanger and $\phi^f_{t-t_0}(v_0)$ is the flow vector of function f satisfying $\frac{\partial}{\partial t}\left(\phi^f_{t-t_0}(v_0)\right) = f\left(\phi^f_{t-t_0}(v_0)\right)$. The variable x is a position of a certain point in the flowing water. Let's define a so called resident time

$$\tau(t) = t - t_0, \tag{3.29}$$

where t_0 is a solution of

$$w(t_0) = w(t) - x, \tag{3.30}$$

which comes from 3.28 under the assumption $x_0 = 0$. If we differentiate the Eq. 3.30 and substitute from 3.29 we get an ODE expressing the time change of the resident time

$$\frac{\partial \tau}{\partial t} = 1 - \frac{u(t)}{u(t-\tau)}\ . \tag{3.31}$$

The temperature profile of the water withing the heat exchanger depends on the resident time. Eq. (3.31) described, how the resident time of the currently leaving water is continuously changed. The resident time is actually what we need to handle in sake of control of output water temperature or heat flow.

3.4.2 Control law

The control problem statement is to find a controller of a form

$$\dot{\zeta} = g(\zeta, e) \tag{3.32}$$

$$u(t) = \phi(\zeta, e), \tag{3.33}$$

where u(t) is the manipulated variable ($\dot{m}$ in the HX case), $e = y - r$ is the control error and ζ the controller state vector. Denote $u_\tau = u(t - \tau)$ and let's have a function $\psi(e)$ so that $e\psi(e) > 0$ (ψ has a same sign as e). Then for input

$$u = u_\tau + \theta\psi(e) \tag{3.34}$$

the error dynamics is asymptotically stable, where $\theta = \text{sign}(L_f h)$. The control law is defined as

$$\dot{\zeta} = \theta\Gamma\left(\|\left(u - \zeta\right)\zeta\| + \|\dot{e}\|\right)\text{sg}(e) \tag{3.35}$$
$$u = \zeta + \theta\psi(e), \tag{3.36}$$

where

$$\text{sg}(e) = \begin{cases} 1, & \text{if } e \geq 0 \\ -1, & \text{if } e < 0. \end{cases} \tag{3.37}$$

The controller state ζ is an esteem of the steady-state control input u_s. For a particular $\psi(e) = k\,e$ the controller changes into

$$\dot{\zeta} = \theta\Gamma k\,|\zeta| + \theta\Gamma\,|\dot{e}|\,\text{sg}(e), \tag{3.38a}$$
$$u = \zeta + \theta k e. \tag{3.38b}$$

3.5 Sandoval Q controller

The advantage of the Sandoval controller is, that it can be used for control of any variable, which depends on states in a single axial point. The heat Q depends on the outlet water temperature T_{wo}, which is a variable depending on a state in an axial point $x = 1$. Hence we can use the Sandoval controller for the Q control as well; The controller input is then the estimated Q according to Eq. (2.39), only the constants k, Γ have to be tuned to different values than in the T_{wo} control case.

3.6 Sandoval Q_r controller

The relative heat flow Q_r can be controlled by the Sandoval controller, as well as the absolute Q.

Chapter 4

Testbed

4.1 One-pipe heating system

In most of the buildings, a two-pipe heating system (schematically illustrated in Fig. 4.1a) is usually used to supply thermal zones (rooms) with hot water. Two-pipe system means, that a supply-pipe and a return-pipe are connected to a boiler and radiators are connected to these tubes in a parallel manner. Through the supply-pipe hot water to heat exchangers is delivered; Through the return-pipe the cooled water is drained back to the boiler to be heated up again. A central pump is used to circulate the water.

The amount of heat transmitted to the thermal zone depends on a mass flow of water through the heat exchanger. The mass flow is nowadays mostly controlled by opening of a control valve. If the user wants to turn-off the heating in one room, the valve has to close to avoid hot water to flow through. Not a long time ago an improved system came into use. Instead of only one central pump and several control valves, there is a pump attached to every radiator. Even in this system a shut-off valve has to be used to stop heating in a specific thermal zone because a turned-off pump still allows the flow to get through.

A different approach is to use a one-pipe system (scheme shown in Fig. 4.1b). This concept uses both ends (supply and return) of a radiator circuit connected to only one central pipe. If the distance between the entering and leaving point is small enough, the difference of pressures is negligible and no water flows through the loop if the pump is not running. The idea is to minimize the distance between the two points in the central tube where the supply and return pipe of the radiator circuit is connected. Let's call this

type of connection a double-T segment. Every radiator circuit consists of a radiator, a control pump and a double-T segment (a connection with the central pipe).

The testbed described in this paper is a realization of a simple one-pipe system. It involves a loop with the central pipe, a central pump and a boiler (primary circuit) and only one radiator circuit (secondary circuit).

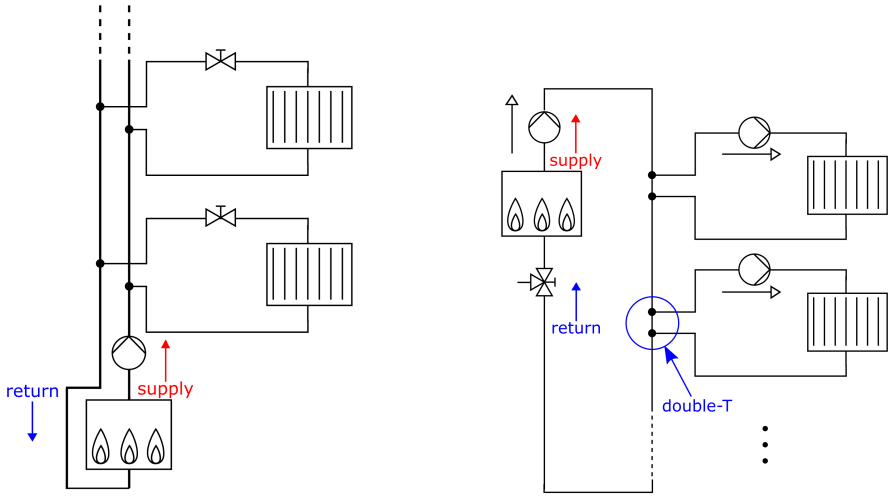

(a) : Two-pipe system scheme **(b) :** One-pipe system scheme

Figure 4.1: 1- and 2-pipe systems

4.2 Testbed construction

For the sake of testing the designed controller on a physical device, a testbed with a one-pipe system and single heat exchanger was built. This section describes the electrical and mechanical construction, used actuators and sensors and the communication with Simulink being run on a PC. The testbed is shown in Fig. 4.16 placed at the end of this chapter.

4.2.1 Mechanical construction

The testbed consists of a primary and a secondary circuit. The primary circuit contains a pump and a boiler and it is used for heating the water and transporting it to the point

where the hot water could be handled by the secondary circuit. The secondary circuit consists of a pump, heat exchanger, valve and a safety valve. Several sensors are placed in the secondary circuit such as the flow-meter, manometer and temperature sensors. The testbed is schematically depicted in Fig. 4.2.

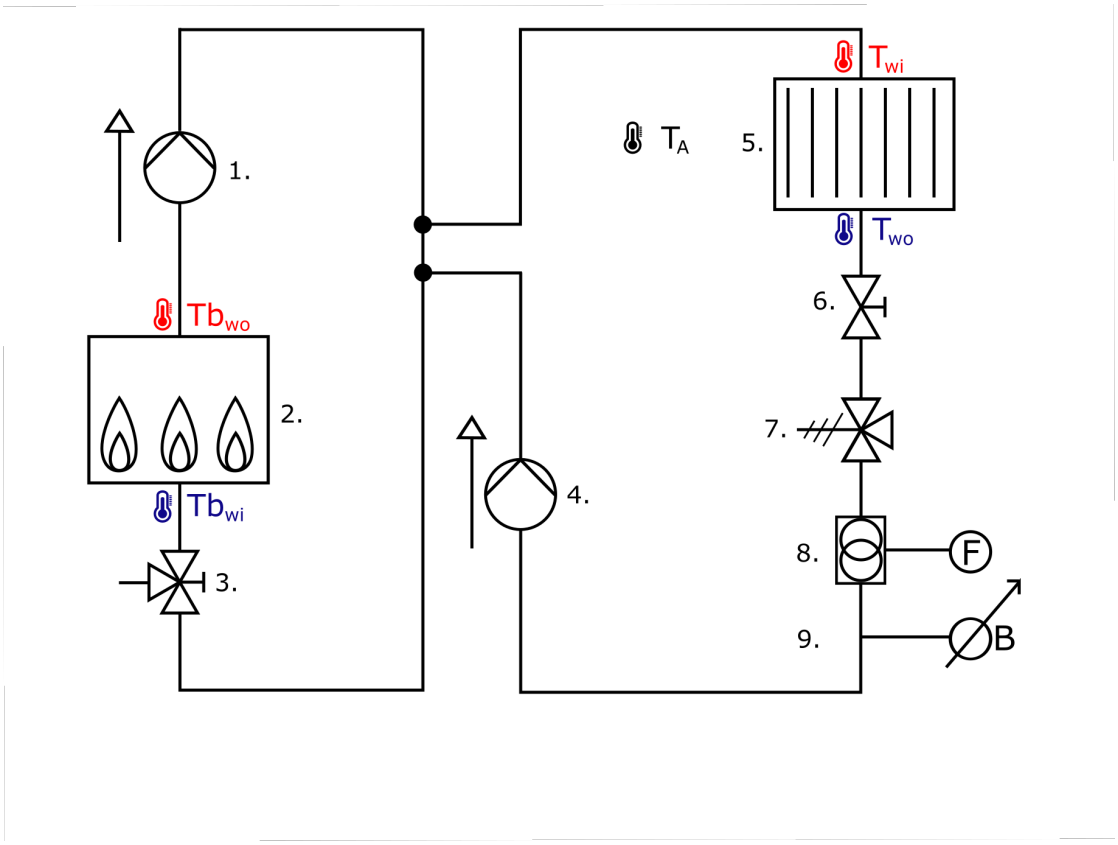

1. *Pump in the primary circuit,* 2. *Boiler,* 3. *Valve,* 4. *Pump in the secondary circuit,* 5. *Heat exchanger,* 6. *Valve,* 7. *Pressure relief valve,* 8. *Flow-meter,* 9. *Manometer*

Figure 4.2: Testbed scheme

4.2.2 Electronics

The electrical part of the testbed is hidden in two cases. One case covers the voltage sources and the second an Arduino board. Several components of the testbed need different supply voltages (listed in table 4.1), therefore it was necessary to use three voltage sources.

Voltage	Supplied components
$12V$ ⎓	Arduino board, Flow-meter
$24V$ ⎓	Pump
$24V\sim$	Valve actuator
$230V\sim$	Boiler

Table 4.1: Supply voltages

As a "brain" of the testbed, which receives signals from sensors and sends signals to actuators, the **Arduino Mega 2560** board was chosen. The advantage of this solution is, that Arduino is widely used among professionals as well as among non-professionals, hence there is a variety of examples and solved problems available. Another advantage is a **Simulink Support Package for Arduino Hardware** offered for Matlab/Simulink, which involves tools prepared for communication between the Arduino and the Simulink.

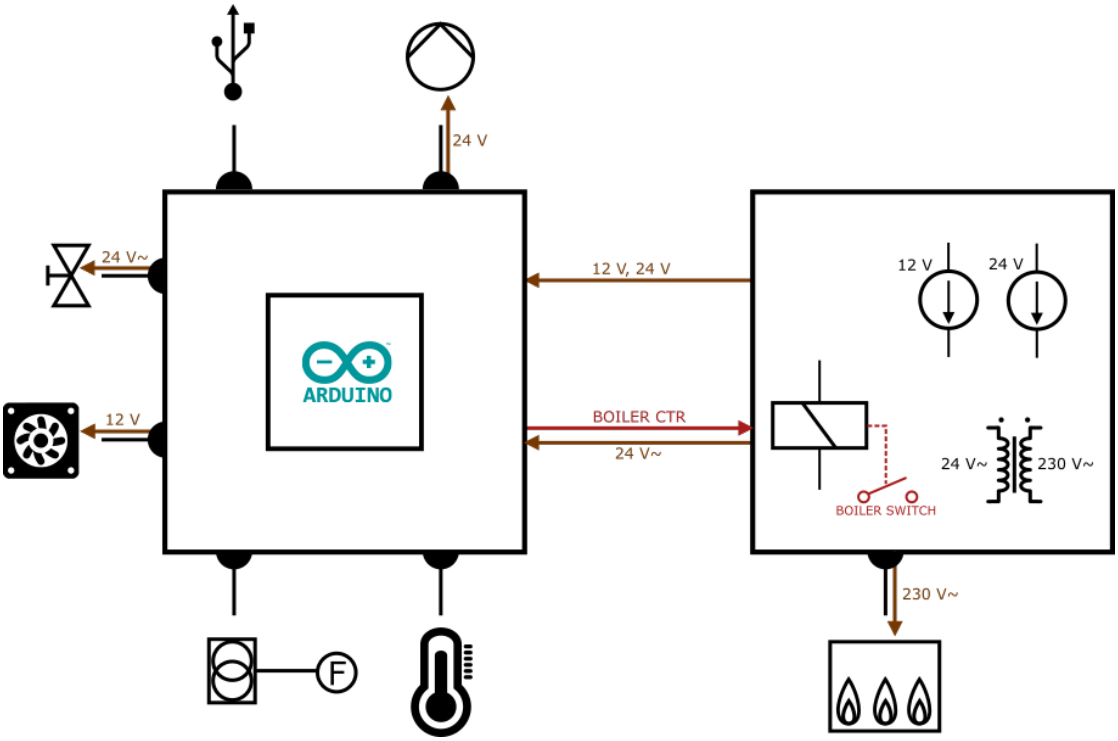

Figure 4.3: Testbed electrical scheme

4.2.3 Actuators

The majority of actuators used in the testbed are controlled electronically which makes it useful also for observing the control values by computer and for logging these values for the later management. However there is a couple of actuators governed manually, but these are valves used almost only during the water filling procedure, which is not part of the experiments.

Pump in primary circuit

Figure 4.4: LOWARA ecocirc BASIC 25-4/130

Pump used to ensure the water flow in the primary circuit is **LOWARA ecocirc BASIC 25-4/130**. This pump is controlled manually and a user can choose from 7 different speeds or pressure stages.

Power:	42 W
Power supply:	Single-phase 200-240 V, 50/60 Hz
Max. mass flow:	3200 kg/h
Control:	Manual, 7 speed/pressure stages

Table 4.2: Pump LOWARA spec.

Boiler

Water heating is provided by a boiler **Leov AD-5** placed in the primary circuit. The boiler could be turned off manually, but the power supply is controlled digitally and a

Figure 4.5: Leov AD-5

PWM control of the heat power was implemented. Fig. 4.6 shows the boiler characteristics measured by an external watt-meter. The characteristics can be considered as linear. For our experiments it is desirable to have a possibly constant temperature of the boiler outlet water, which was described in the control chapter in section 3.1.

Capacity:	5 l
Power:	1000 W
Power supply:	Single-phase 200-240 V, 50/60 Hz
Control:	PWM, 2 Hz

Table 4.3: Boiler Leov spec.

Pump in secondary circuit

Water circulation in the secondary circuit is ensured by a pump **Alphacool VPP655-PWM**. Speed of the pump is controlled by a PWM signal and its real speed can be measured by pulses sent by the pump per every revolution.

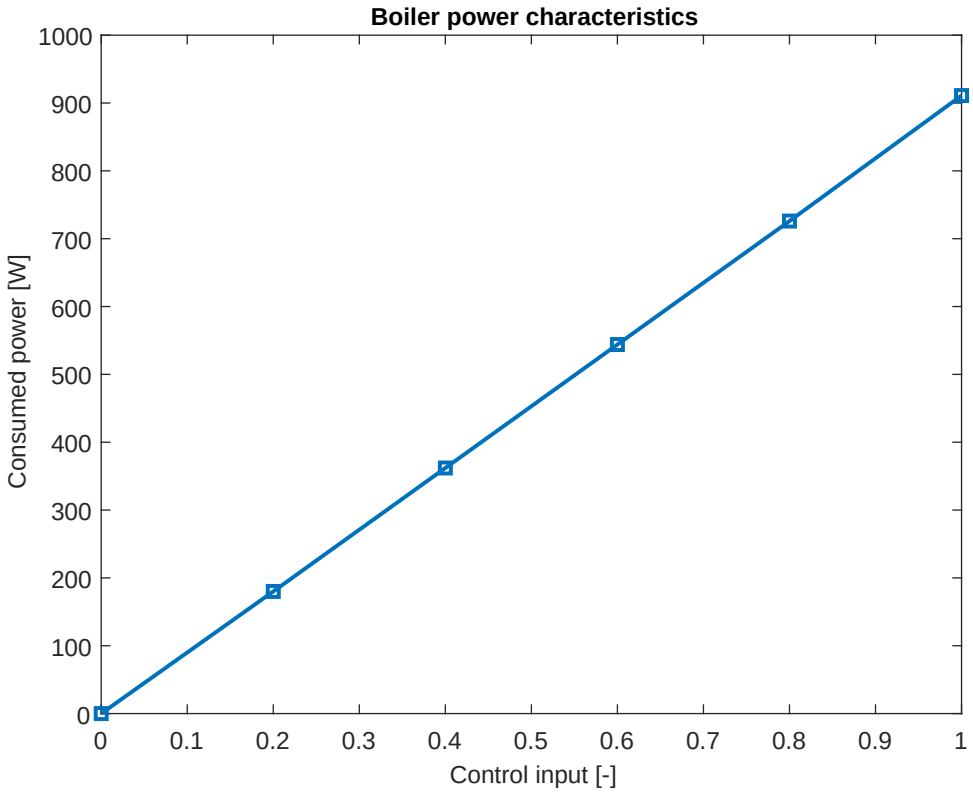

Figure 4.6: Leov boiler power characteristics

Power:	37 W
Power supply:	12V DC
Max. flow:	1500 L/h
Control:	PWM signal, rated voltage 8-24 V DC, 400 Hz
Revolution monitoring:	Pulse signal

Table 4.4: Pump Alphacool spec.

Heat exchanger & fans

Although the heat exchanger alone should not be considered as an actuator, there are fans (Fig. 4.8b) mounted on it. The speed of the fans can be governed by a PWM signal which rapidly changes the heat transfer properties of the heat exchanger. The properties

Figure 4.7: Alphacool VPP655-PWM

of the heat exchanger were introduced in chapter 2.

(a) : Watercool MO-RA3 360

(b) : Prolima TECH Vortex 12

Figure 4.8: Heat exchanger

Power:	1.44 W
Power supply:	12 V DC
Max. airflow:	95 m^3/h
Control:	PWM signal

Table 4.5: Fan spec.

Valve actuator

In the testbed there is a valve whose opening and closing can be initiated electrically. For that sake, the **Honeywell M6410C2320** actuator is used. A purpose of this element is to change a hydraulic resistance of the secondary circuit during a simulation.

Figure 4.9: Honeywell M6410C2320

Power:	0.8 W
Power supply:	24 V AC
Stroke:	6.5 mm
Running time:	150 s (at 50 Hz)

Table 4.6: Honeywell M6410C2320 spec.

4.2.4 Sensors

Mainly, electronically communicating sensors are used in the testbed, only a dial manometer was placed to the testbed to enable a visual pressure-check.

Flowmeter

The volumetric flowmeter **B.I.O.-Tech 150175** measures the water flow in the secondary circuit. The output of the sensor is a pulse signal; 80 impulses strike one liter. The value of $\dot{m}$ $[kg/h]$ are computed as

Figure 4.10: B.I.O.-Tech 150175

$$\dot{m} = \frac{3600}{N_{imp} \cdot 10^{-6} \cdot \tau_{\dot{m}}} \rho_w, \tag{4.1}$$

where $\tau_{\dot{m}}$ $[\mu s]$ is the number of microseconds between two pulses received from the flowmeter, $N_{imp} = 80$ $[imp/l]$ is the number of impulses per one liter and ρ_w $[{}^{kg}/_{m^3}]$ is the water density.

Measure principle: turbine
Range: 0.5 - 50 L/min
Power supply: 4.5-24 V DC
Output signal: Pulses, 80 Imp./Liter

Table 4.7: B.I.O.-Tech 150175 spec.

Temperature sensor

There are six temperature sensors used in the testbed. They measure temperatures of the boiler inlet water T_{bi}, boiler outlet water T_{bo}, heat exchanger inlet water T_{wi}, heat exchanger outlet water T_{wo}, inlet air T_{ai} and outlet air T_{ao}. The temperature sensor used is **Texas Instruments LM35CAZ**, which is a sensor with analog output.

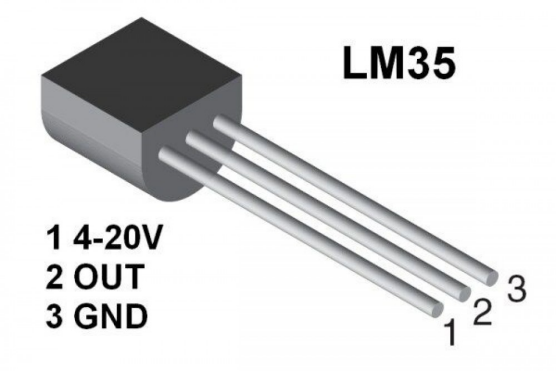

Figure 4.11: LM35 CAZ

Range: -40 $°C$ to 110 $°C$
Power supply: 4-30 V DC
Output signal: analog, voltage 10mV/°C

Table 4.8: LM35 CAZ spec.

Manometer

Figure 4.12: Manometer Ferro

This sensor shows a value of the water pressure in the testbed. The range of the used manometer is 10 bars and it is placed in the secondary circuit. The measured value is

not stored in the computer, the sensor serves only for a visual check of the water pressure inside the testbed. It is important to know the pressure to avoid a damage of components of the testbed. The pressure has to be check not only during the filling procedure, when the pressure can reach a degree of pressure used in a water supply network (cca 4bar), but also during experiments due to a pressure increase caused by heating.

4.2.5 Simulink-to-Arduino interface

For the controller development and testing, it is necessary to run the Hardware-in-the-loop simulation so that we can access the real-time measured variables and to run part of the computations on computer. For this purpose the usage of *Simulink Support Package for Arduino Hardware* is suitable. The communication process scheme is depicted in Fig. 4.13. Arduino reads data from sensors and sends it via serial line to the computer, where the Simulink simulation runs. According to the received data, Simulink computes the control signals and sends it back to Arduino, which writes it to the actuators. No control algorithms are executed in Arduino due to computation demands.

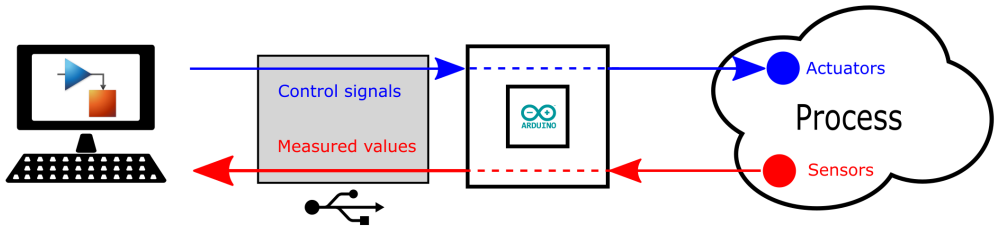

Figure 4.13: Communication via Arduino

Simulink Support Package for Arduino Hardware

This library is a tool to design a control algorithm in the Simulink environment, download it to the Arduino board and then run it in a stand-alone mode or in an external mode, which allows us to observe the process variables in real time and also to log these data into Matlab workspace. Although it is easy and fast to implement the control this way, but there is a big drawback, that the whole program has to be computed by the Arduino, and Simulink works only as a scope.

The library contains blocks for reading the digital and analog inputs, for writing into the digital outputs and also for PWM output. A handicap of the PWM output block is that it provides only the frequency 490 Hz and it is not possible to change it. There is

an opportunity to use an S-Function block that interprets a C code and is the way how implement a PWM with custom frequency. Similar block was used for reading the data from flow-meter as well, because of the need to use an interrupt service routine triggered by the rising edge of the pulse signal from flow-meter.

Serial port communication

First, we tried to design the control system in one Simulink file, then download it to the Arduino board and run it in external mode. The external mode allows users to access the controlled and measured variables in a real time manner. The whole computing is accomplished in the Arduino board which is a bit inefficient, when the PC is available anyway. Even though our simulink model was not a difficult one, it showed up the Arduino was not capable to finish the computations on time and the simulation often crashed.

After several unsuccessful attempts to simplify and bring the model into a stable form, we decided to use the Arduino board only as an I/O board and the other computations execute in the Simulink model on PC. The transfer of data between the PC and the Arduino board is performed via serial line by USB.

The Arduino library for Simulink contains a Serial Transmit block (Fig. 4.14) that allows to read and write data from/to the serial line. In the newest version it allows the user to select a data type of the sent/received variables and a number of variables to be transferred. It works well on the Arduino side; The data sent from computer to Arduino are received properly and also data sent from Arduino to computer are buffered in the serial line. However on the PC side the manipulation with the received data is a little tricky. Hence custom system object blocks (Fig. 4.15) were implemented for handling the communication.

The Simulink simulation runs with certain time steps which do not necessary correspond to the real time. But for a real-time communication, we need the real timing both for Simulink and Arduino. To solve this, a Real-Time Pacer was used in the Simulink model. The Real-Time Pacer manages to run a real-time simulation and to read/write data in a specified time intervals. The actual computation task is accomplished and the remaining time from the sampling period is filled with a Matlab pause function. It is not a very elegant solution, but it works.

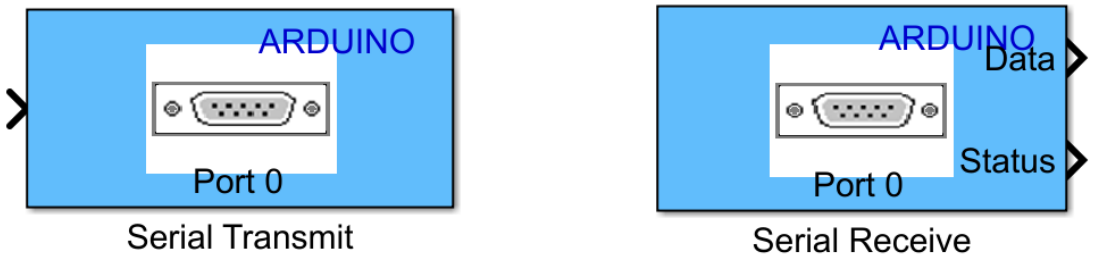

Figure 4.14: Serial transmit blocks

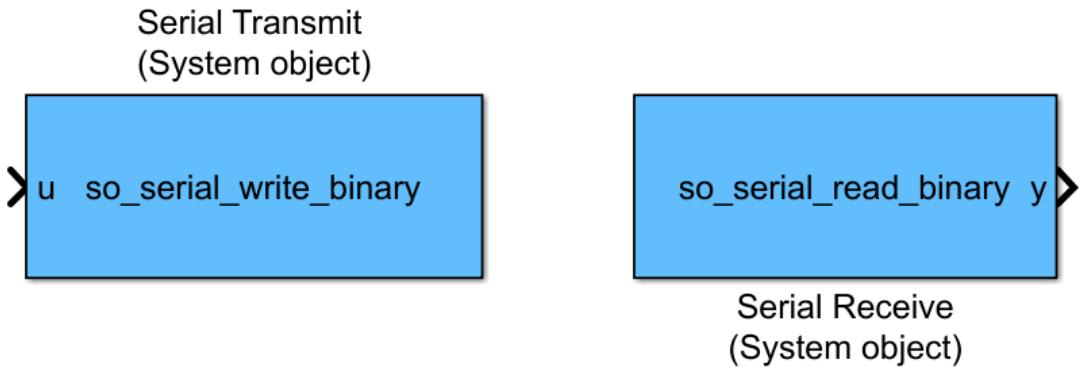

Figure 4.15: Custom serial transmit blocks

4.3 Testbed limits

There are several technical limits constraining the experiments performed on the testbed. The main constraint is the maximal power the boiler can provide, which is nominally 1000 W, but the value we measured is $Q_{bMax} = 920\,\mathrm{W}$. It gives an upper bound to Q_{SP} we can require.

Another restriction is caused by the lower bound of a range of the flow-meter, which is $0.5\,\mathrm{L\,min^{-1}} = 30\,\mathrm{kg\,h^{-1}}$. It is still too much for the desired small heat flows, which we need to achieve a low HX heat. Both these bounds cause, that the range of set-point values of Q_{SP} we could use, is a little bit narrow.

Figure 4.16: Testbed

Chapter 5

Experiments

5.1 Simulation experiments

This section presents the results obtained by the Simulink simulations of a heat-exchanger system controlled by the proposed controllers.

5.1.1 Shang T_{wo} controller

This test compares three ways of the outlet water temperature control. A PI controller, the Shang controller and the Shang controller with an integral part. Fig. 5.1 shows the simulation results. The Shang controller without an integral part is able to reach the set-point value with a satisfactory small offset (with a proper knowledge of UA of the system). However there is a small overshoot by using the Shang controller with an integral part, it is able to reach the set-point value faster and more accurate than the simple Shang controller. On the other hand, the results of the PI controller are significantly poor. It is possible to tune the controller for some set-point, which can be reached almost promptly, but for the further set-points it either oscillates or is too slow to reach the reference value.

5.1.2 Sandoval T_{wo} controller

Next simulation experiment was a test of the Sandoval T_{wo} controller. The temperature of the inlet water was $T_{wi} = 47°C$ and the set-points were a stairs sequence. The results are shown in Fig. 5.2. The Sandoval controller is able to drive the system output to the set-point value significantly faster, than the PI controller does.

5.2 Testbed experiments

We ran several experiments on the testbed, to check the controllers also on a physical system. Some of them are presented in this section. For all experiments, the boiler output water temperature was driven and sustained at 47 °C, which corresponds with the heat exchanger water inlet temperature T_{wi}. The output water temperature T_{wo} can reach a value from range $(T_{wi} - T_{ai})$, where the room air temperature was usually T_{ai} around 22°C or 23°C.

5.2.1 Model identification

The Shang controller illustrated in section 3.2 requires the knowledge of the heat transfer coefficient, which was unknown. Hence we were supposed to run an experiment to find this coefficient. It was important to keep the system possibly in a steady state for a while and to measure the temperatures of inlet water T_{wi}, outlet water T_{wo} and of the surrounding air T_{ai}. Next, the information about the mass flow $\dot{m}$ was demanded. The value of UA is computed according to Eq. (2.7).

The temperature of the water in the boiler and the outlet water from heat exchanger were controlled by a Shang controller with an integral part. The UA value needed as a parameter of this controller was roughly estimated from previous experiments. The UA value was found for two different settings, one with two fans running (Fig. 5.3) and with three fans running (Fig. 5.4). The first plot of the figures shows the T_{wo} value with the instantaneous UA value. It is important to possibly choose steady state values, so the chosen time slots are marked with a red color. The UA value is computed only for these time slots. The second plot depicts a linear approximation of UA on mass flow (Eq. 5.1)

$$UA \approx a_1 \dot{m} + a_0. \tag{5.1}$$

It can be seen, that adding another fan has a significant influence on the heat transfer rate.

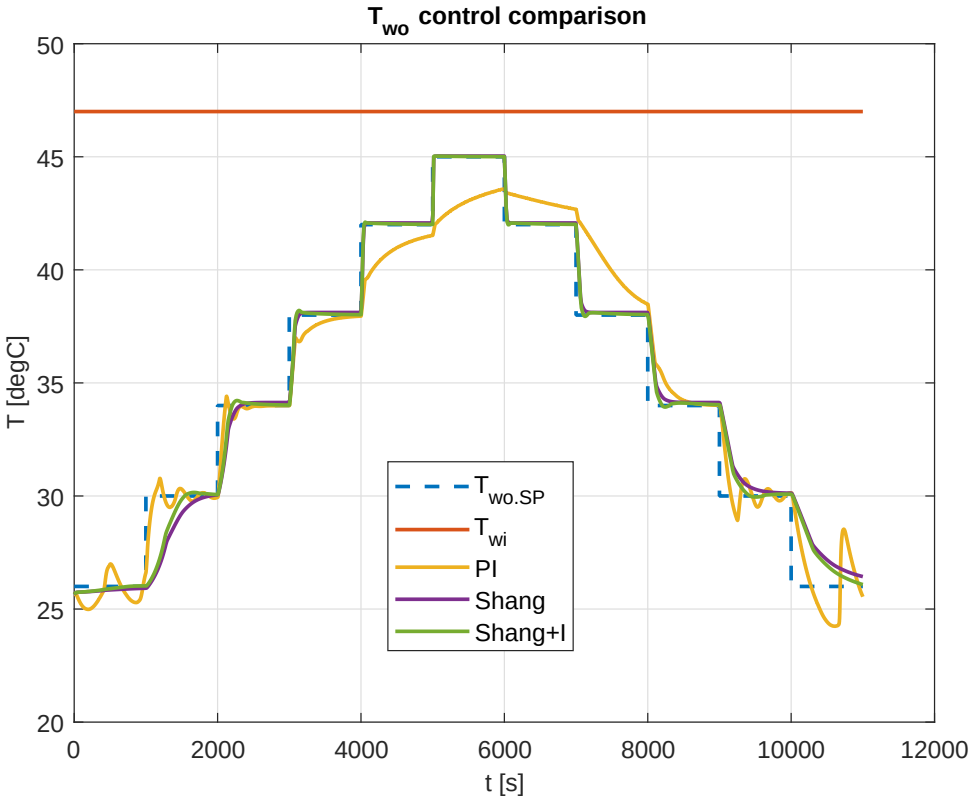

Figure 5.1: T_{wo} controllers comparision

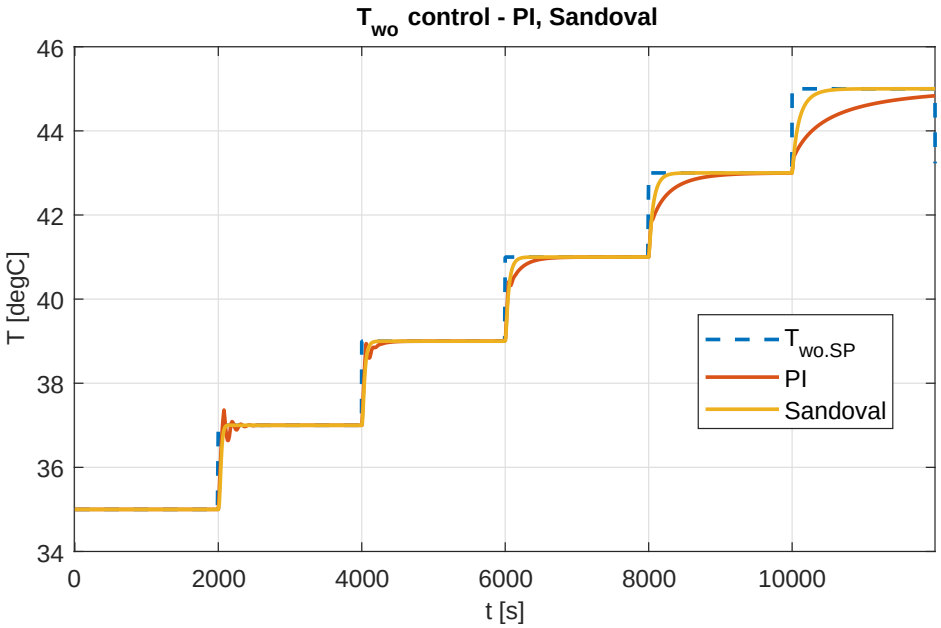

Figure 5.2: T_{wo} controllers comparision

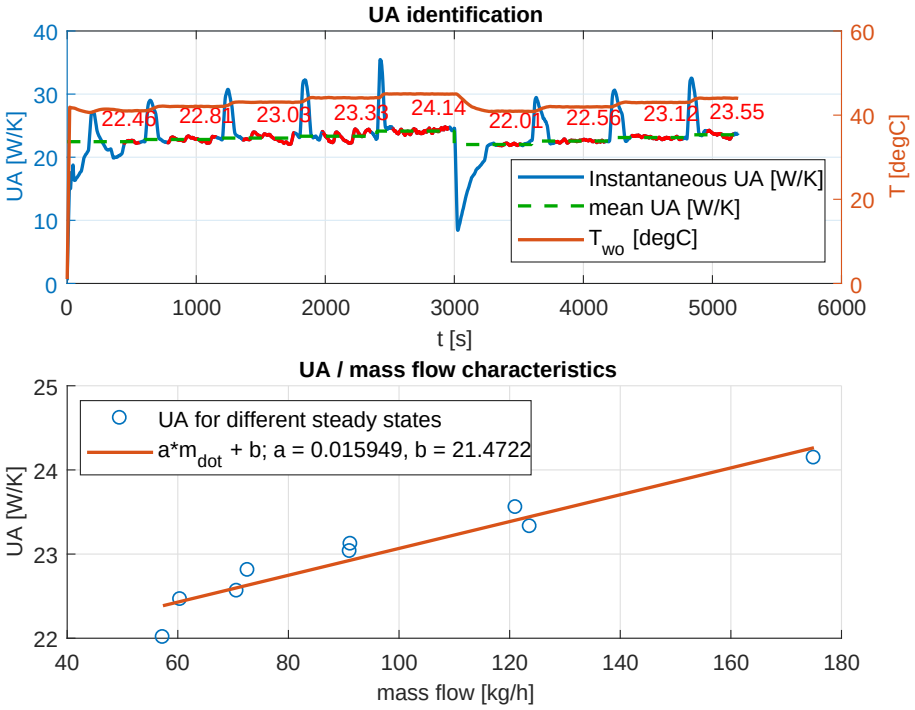

Figure 5.3: *UA* identification for a 2-fans heat exchanger

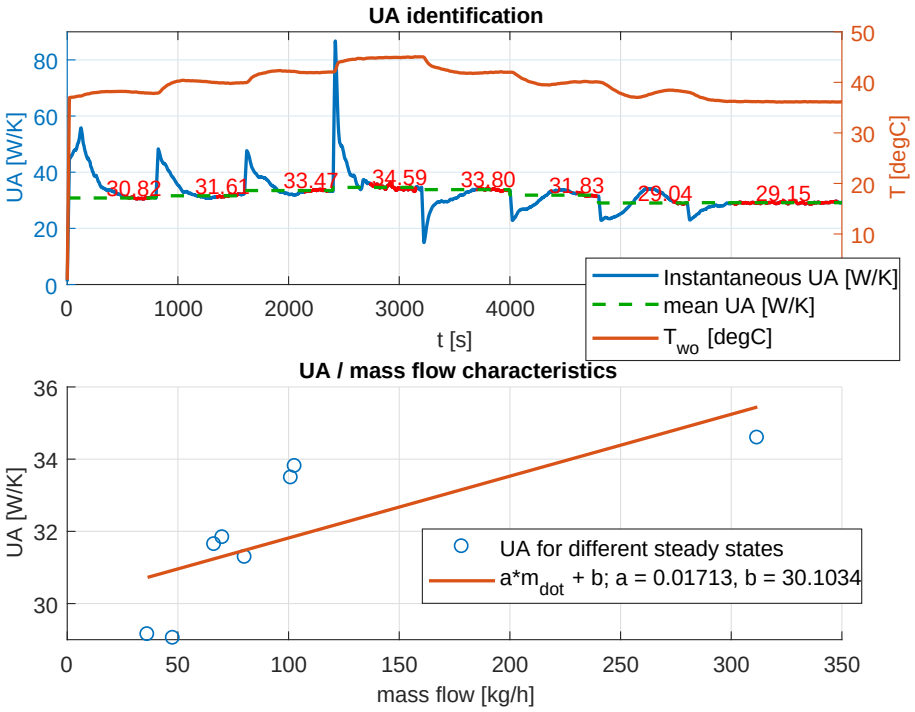

Figure 5.4: *UA* identification for a 3-fans heat exchanger

5.2.2 T_{wo} Shang controller

This experiment tested the Shang controller; This controller requires the knowledge of the heat transfer rate UA, which was found by a previous experiments. Results of this experiment are depicted in Fig. 5.5. The reference given to the controller was a stairs sequence of $T_{wo.SP}$ values. The inlet air temperature T_{ai} was 25.5 °C and the set-point for the inlet water temperature was set to 47°C, which defines the range for T_{wo} to be [25.5–47].

Obviously, the Shang controller without an integral part has a steady-state offset, because we only approximate the value of UA. The set-point $T_{wo.SP} = 45$°C between times 3200 s and 4000 s was not achieved due to too high heat transfer rate UA (all three fans were running at 100%) and the boiler was not able to heat water enough. If we do not take into account the set-point $T_{wo.SP} = 45$°C, then the biggest steady state offset was 0.54°C for the set-point $T_{wo.SP} = 40$°C, which is 2.3% of the range.

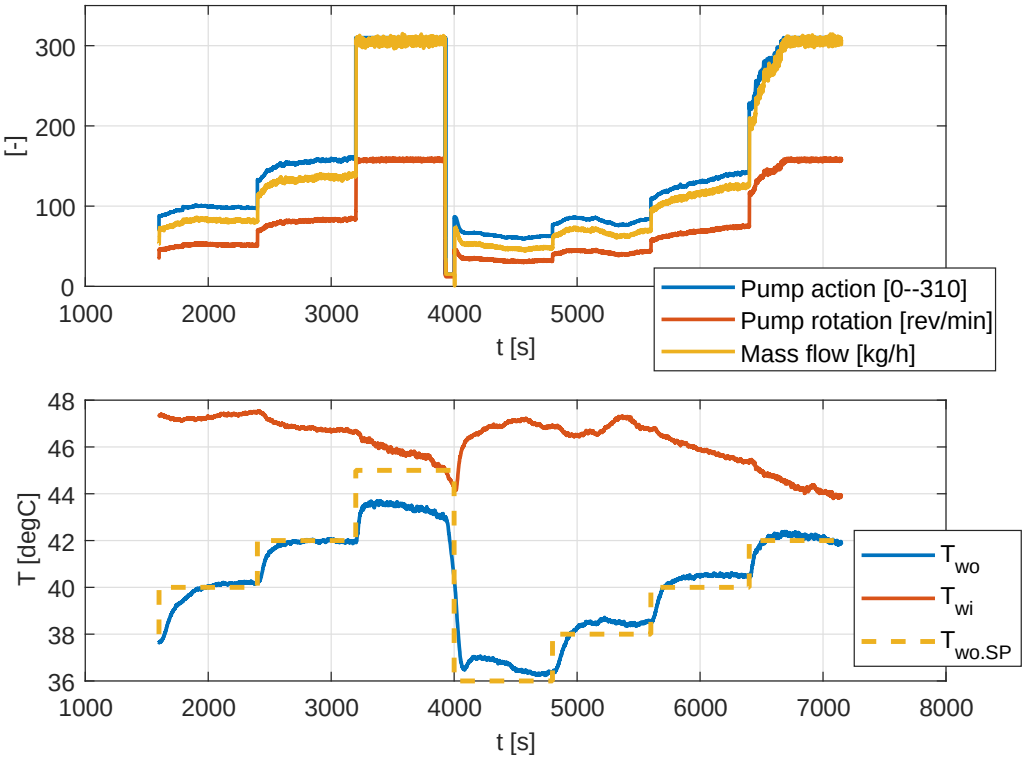

Figure 5.5: Shang control of T_{wo}

5.2.3 T_{wo} Shang controller with an integral part

In this simulation, the outlet water temperature T_{wo} was controlled by a Shang controller with an integral part. The reference given to the controller was an up-going and down-going stair sequence with values between 36 °C and 45 °C. This time, only 2 fans were running.

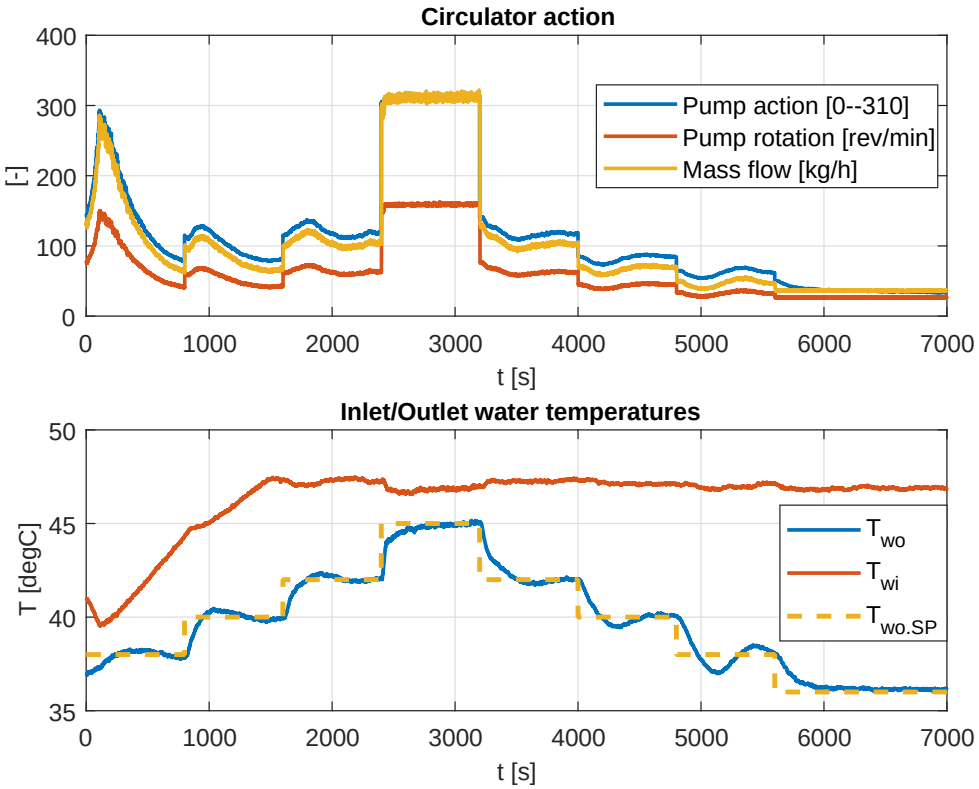

Figure 5.6: Shang+I control of T_{wo}

Fig. 5.6 depicts measurement results. The first plot contains pump data, the control signal sent from computer, pump revolutions rate measured by pump itself and a mass flow measured by a flow-meter. The second plot displays temperatures of the heat exchanger inlet and outlet water. The controller was satisfactorily able to achieve and hold the controlled output at the reference value, even with a changing T_{wi}. Next, the control at the higher ref. values was faster and more accurate, because the system worked with a higher mass-flow, which makes it easier to control. The steady-state offsets are almost zero. The biggest overshot was 0.41°C (1.9% of range) for the set-point step from 38 °C to 40 °C. The biggest undershot was 0.98°C (4.6% of range) and occured during the set-point step from 40 °C to 38 °C.

5.2.4 PI T_{wo} controller

This experiment tried to show a performance of a PI controller in this system. The controller was tuned on a set-point value $T_{wo.SP} = 42\,°\text{C}$. The results are depicted in Fig. 5.7. It can be seen, that if the set-point value is far from the value, which was used for the controller tuning (e.g. $T_{wo.SP} = 38\,°\text{C}$ round time 4000 s), the controlled output starts to oscillate. The biggest overshoot of dimension 5.2°C occured for the setpoint $T_{wo.SP} = 38\,°\text{C}$, which was 24.2% of range.

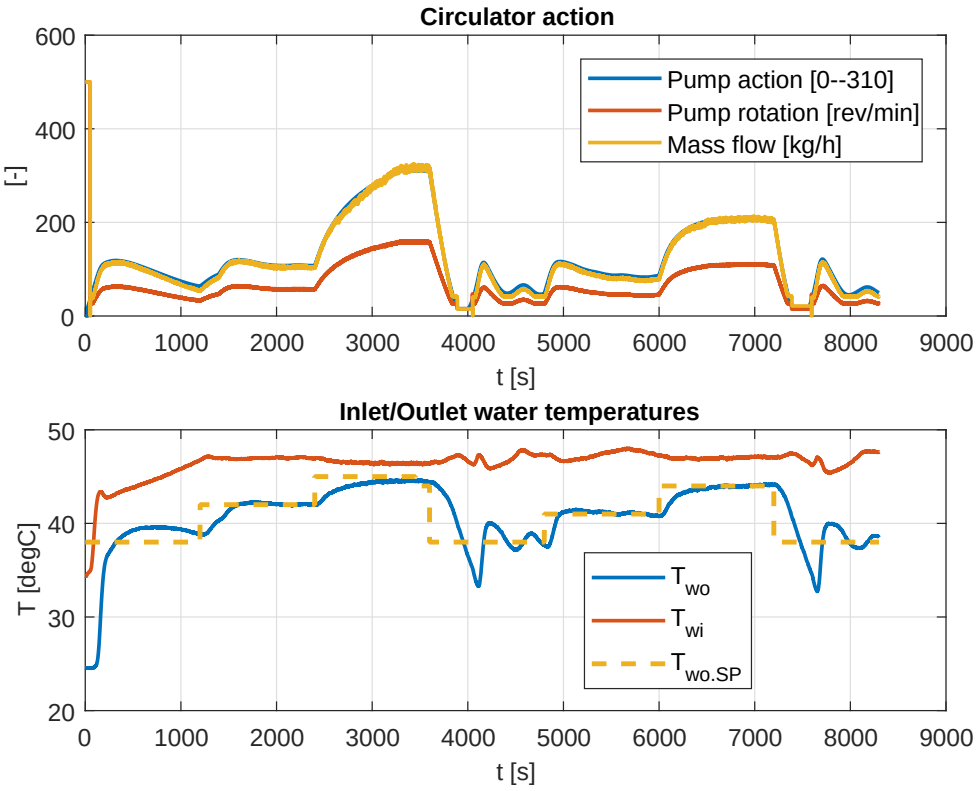

Figure 5.7: PI control of T_{wo}

5.2.5 T_{wo} Sandoval controller

Fig. 5.8 depicts results of a similar experiment as the previous ones, but the Sandoval controller was utilized (introduced in section 3.4). It's advantage is, that there is no need of prior knowledge of the system parameters, namely the UA value, or to know the inlet water temperature T_{wi} or the air temperature T_{ai}. On the other hand, one has no guidance for finding the correct values of the tunable parameters k, Γ. In Eq. (3.38b),

which describes the controller. Both k and Γ are contained in the first equation, so they both contribute to the integral part of the controller. Tuning is therefore not so straightforward as for a PI controller. This controller is able to drive the system

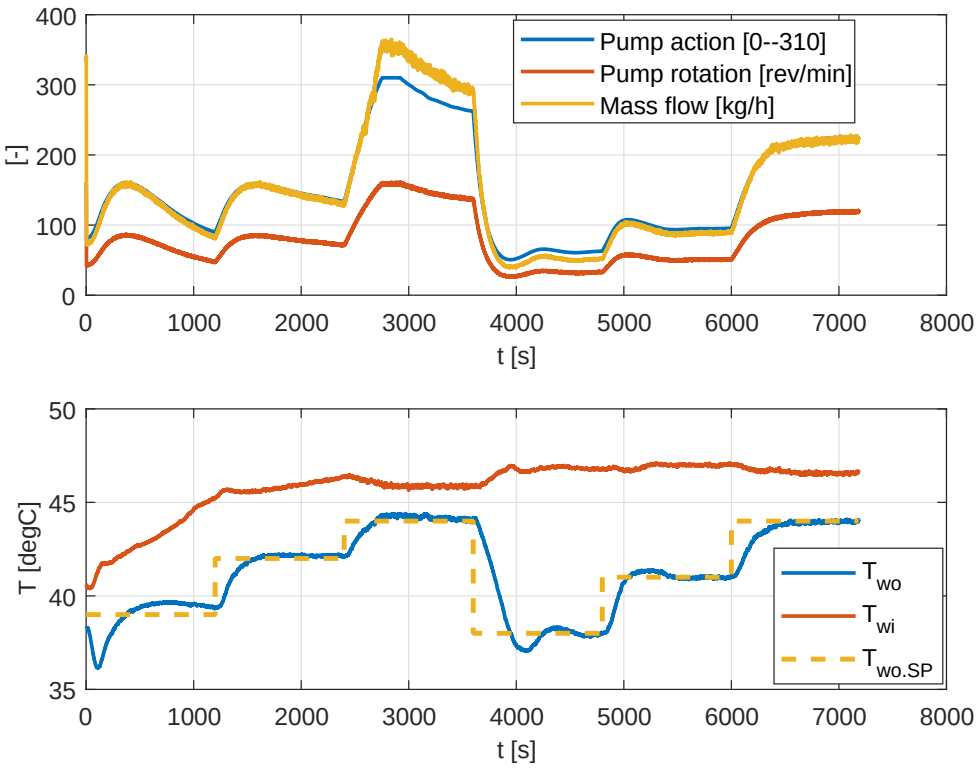

Figure 5.8: Sandoval control of T_{wo}

output to the set-point value with satisfactory small over-shots, even that it has no prior information about the system.

5.2.6 Q Shang+I control, test 1

The heat flow of the heat exchanger was controlled during this experiment. From the heat flow set-point Q_{SP}, the $T_{wo.SP}$ reference was computed according to Eq. (2.29), but instead of a constant UA, a linear approximation based on the results of the previous experiment (second plot in Fig. 5.4) was utilized. However, the approximated value of UA was computed by Eq. (5.1), where for the $\dot{m}$ the actual mass flow value was taken. The last 200 s of the experiment depicted in Fig. 5.9 show, that it was a not a good idea.

Assume that Q_{SP} just changed to a higher one, which demands higher $T_{wo.SP}$ and controller therefore sets higher mass flow. The higher mass flow, the bigger value of UA,

which then induces lower $T_{wo.SP}$ for the same $Q.SP$. But lower $T_{wo.SP}$ means the lower mass flow demanded, which again induces lower UA and the cycle repeats. Exactly this can be seen in the last 200 s of the experiment. In the first plot it seems that the pump speed oscillated through 50 % of its range.

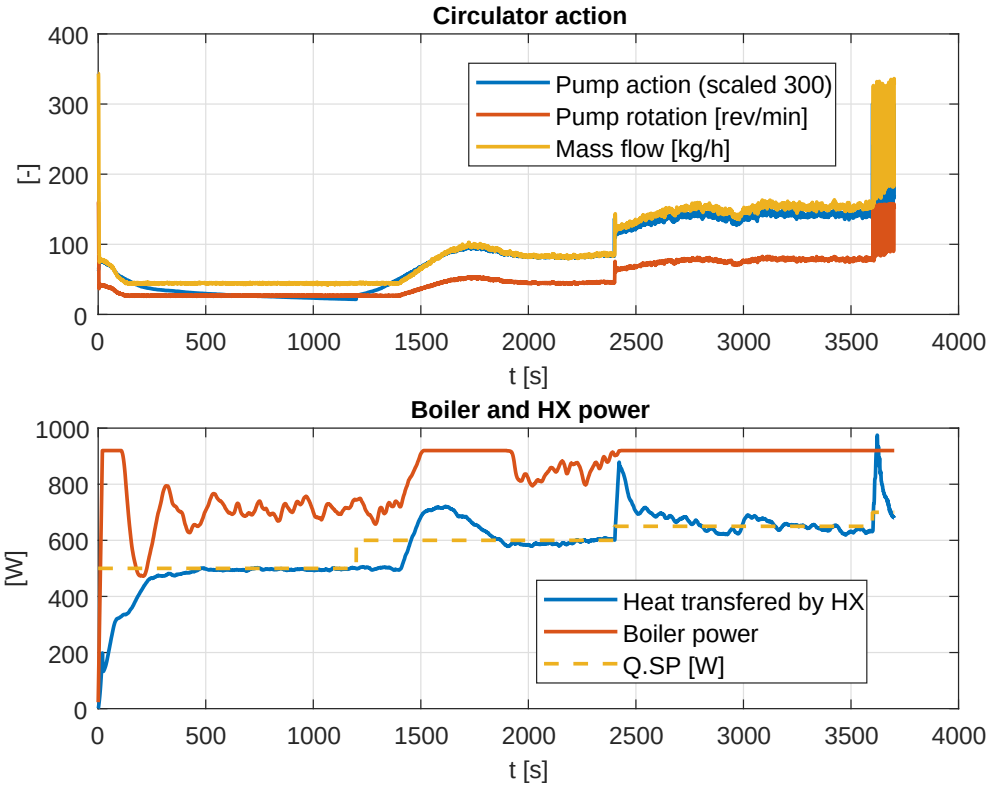

Figure 5.9: Shang+I control of Q, oscillating

5.2.7 Q Shang+I control, test 2

Settings of this experiments were similar to that in the previous experiment, only a different computation method was used for the $T_{wo.SP}$ reference computation. This time, it was computed from the steady-state value of Θ_{out}, which was found as a result of Eq. (2.33) and Eq. (2.34), only the value UA was not approximated exponentially, but linearly. The result of this experiment are shown in Fig. 5.10.

Always, when there is a change in the Q_{SP} value, then during the transient a huge over/undershot appears (e.g. at time intervales $1000 - 1400$ s or $2000 - 2500$ s). It is actually not the real heat flow, but an estimate, which is correct only during the steady state. It is caused by the heat flow estimation method Eq. (2.21). When the set-point is changed to a higher value, the mass flow is increased almost immediately, however

at the heat exchanger output is still water, which has spent more time inside, than it is supposed to, according to the current mass flow. Therefore it is a bit colder, than it would be in a steady state with the new value off mass flow; The temperature difference $T_{wi} - T_{wo}$ is bigger and the heat flows appears to be higher.

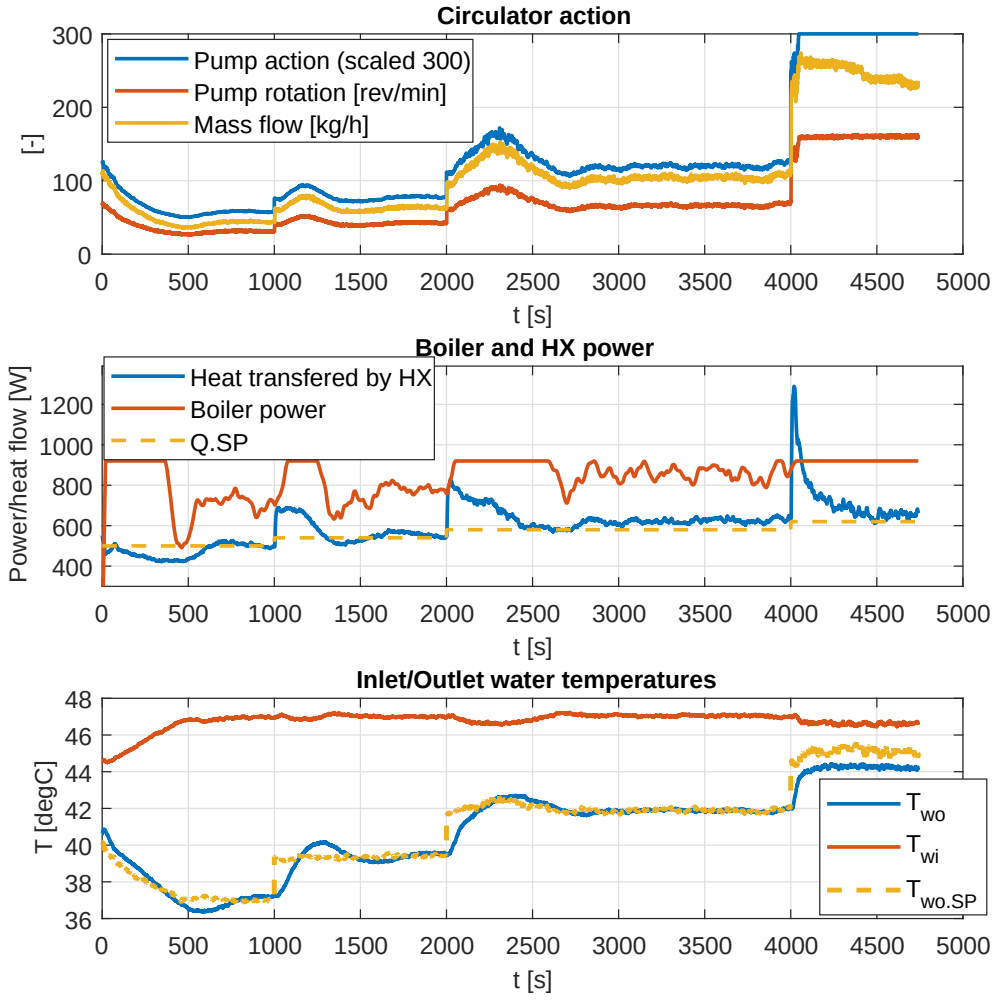

Figure 5.10: Shang+I control of Q

5.2.8 Q Sandoval control

This experiment tested a Sandoval controller used for a heat control. This time, the Q_{SP} was not transformed to the $T_{wo.SP}$, but it was directly assigned to the controller as a reference. The controlled variable was heat Q, which was estimated by a formula in Eq. (2.39). The results of the experiments are shown in Fig. 5.11. The controller is

able to drive the heat flow to the reference value, but again, the range is restricted; The heat flows lower than 500 W cannot be reached and controlled due to the features of the testbed.

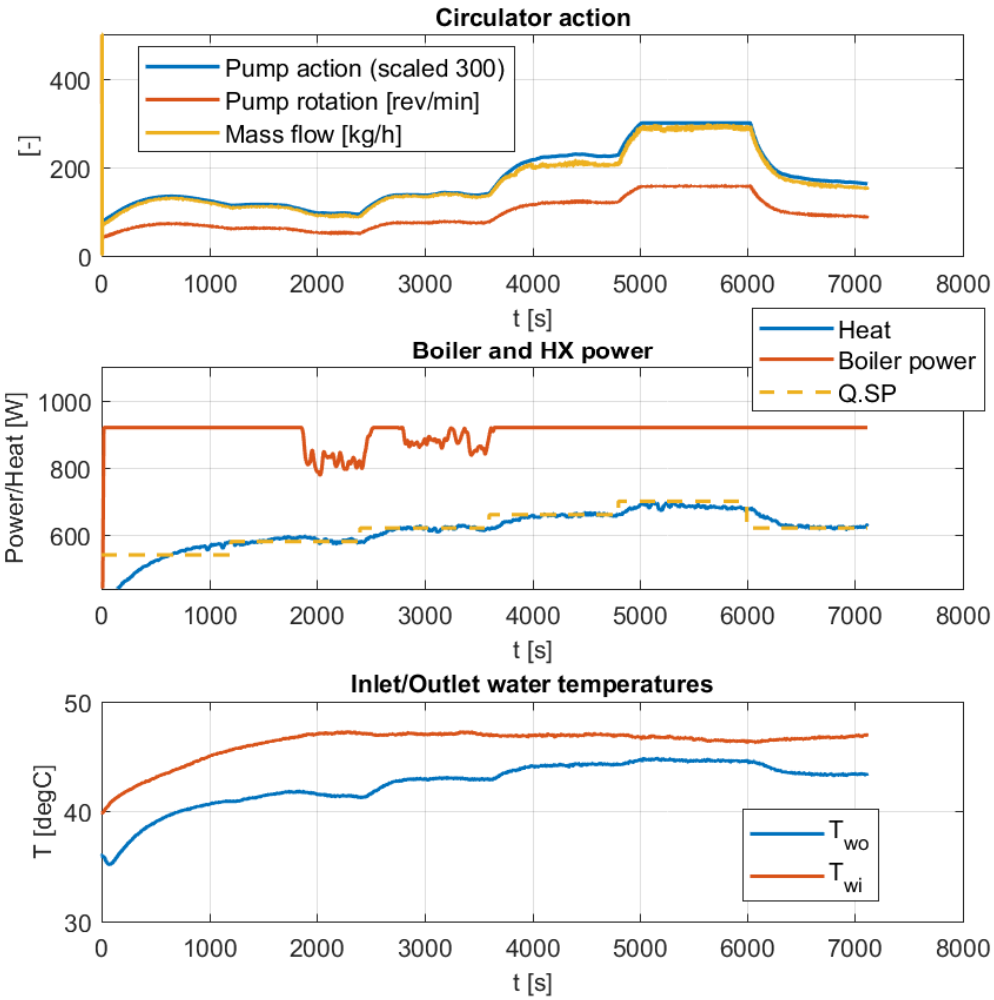

Figure 5.11: Sandoval control of Q

5.2.9 Q_r Sandoval control

Finally, we tested the relative heat flow control as well. The results are depicted in Fig. 5.12. The Q_{max} was arranged to be the heat flow corresponding to the unused water content of value $\Theta = 0.9$. In other words, at least 10% of heat stored in the water should be transferred to the surrounding air. Such a maximal heat flow is $Q_{max} = 623\,\mathrm{W}$. The results show, that both the relative heat flow and the estimated (in plot it is normalized)

are driven to the set-points.

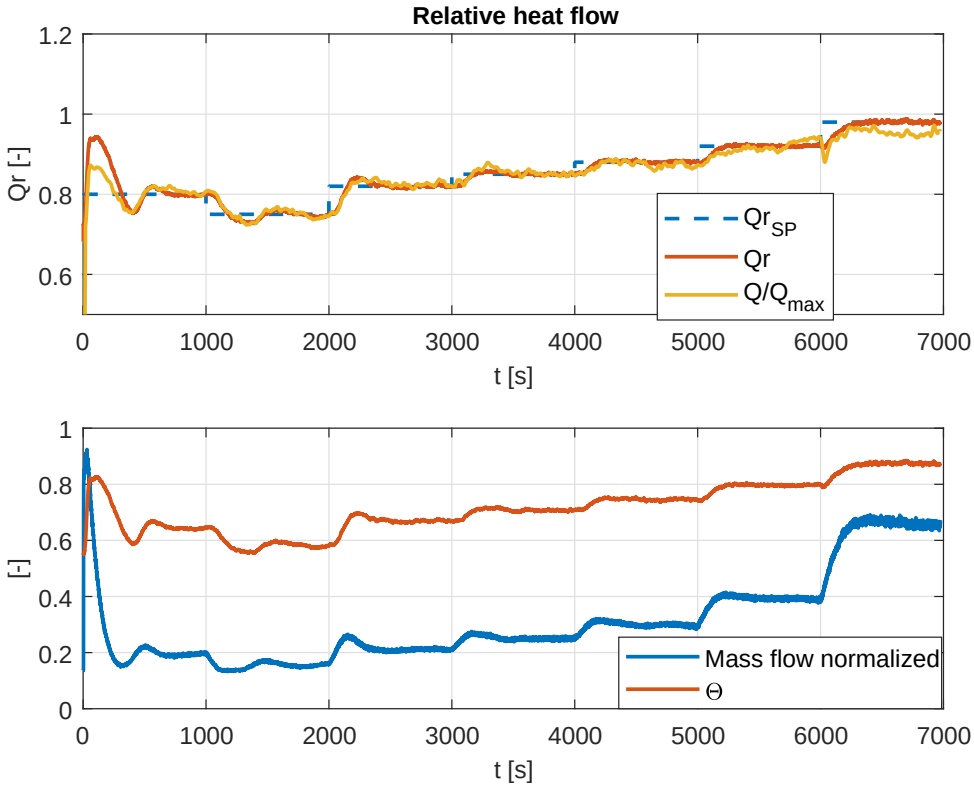

Figure 5.12: Sandoval control of Q

Chapter 6

Conclusion

In this thesis, several controllers for the outlet water temperature T_{wo} and for the HX heat flow Q were described. For the purpose of synthesis and testing, a computer model of a heat exchanger and a physical testbed were built. A couple of obstacles delayed the testbed realization and made the construction difficult; The major delays were caused by an implementation of Simulink-to-Arduino communication, on account of unreliability of the first implemented solution. But despite the difficulties, we managed to complete it early enough to execute experiments on it for this thesis.

The performance of the proposed controllers was tested both by a computer simulation and during the experiments on the testbed. The Shang's controller without an integral part was not able to reach the T_{wo} set-point value without offset, but on the other hand, its reaction was fast. The problem with the steady-state offset disappeared after addition of an integral part, as well as by utilization of the Sandoval's controller. The Shang's controllers require prior knowledge of the controlled system, such as the heat transfer coefficient, surrounding air temperature and the inlet water temperature, while the Sandoval's controller needs only the set-point value and the measured output. The experiments performed on the testbed show, that the proposed control strategies give better results than a PI control. However, the PI control performance was not as poor in the testbed experiments, as we expected. It is likely, that we tested the controllers only within a small range, where the PI controller drawbacks did not appear very much.

We were able to estimate the heat transfer coefficient of the heat exchanger from the identification measurements accurately enough, to successfully tune the Shang's controllers and to be able to transform the heat flow set-point to the outlet water temperature set-point. This transformation was needed for the Shang's heat flow controller. Then an estimated heat flow and relative heat flow were controlled by the Sandoval's controller.

The results were better than in the case of the Shang's heat flow control. The advantage of the Sandoval's relative heat flow control is an absence of necessity to know the heat transfer coefficient.

Moreover, a model of the heat exchanger was an interesting task as well. It is a hybrid model obtained by the Finite Volume Method, which is a technique for a creation of a model described by a set of PDEs. Furthermore, we tried to discretize the continuous part of the model, to obtain a pure discrete model, which would reduce the computation time.

There is still a lot of challenging work to be done on the testbed. It should be redesigned in some aspects; The boiler should be changed for a more powerful one, a flow-meter with a range more suitable for our purposes should be placed. We hope, that we are going to find a suitable solution of the exact discretization of the heat exchanger. Another future goal is an implementation of the heat exchanger temperature profile observer.

Bibliography

[1] Michael Baake and Ulrike Schlaegel, *The Peano-Baker series*, (2010), 1–6.

[2] Davood Babaei and Pourkargar Antonios Armaou, *Adaptive Control of Chemical Distributed Parameter Systems*, IFAC-PapersOnLine **48** (2015), no. 8, 681–686.

[3] B. Bamieh, *Lecture 5 : Continuous-Time Linear State-Space Models 1*, 1999, pp. 1–5.

[4] Panagiotis D. Christofided, *Nonlinear and Robust Control of PDE systems: Methods and Applications to Transport-Reaction Processes*, Birkhäuser, Boston, 2001.

[5] Nils Christophersen and Geir Storvik, *Linear dynamical models, Kalman filtering and statistics. Lecture notes to IN-ST 259*, (1998), no. October.

[6] Jiri Dostal, *Decentralized Control of Hydronic Building Systems*, Ph.D. thesis, CTU in Prague, 2015.

[7] Jiri Dostal and Vladimir Havlena, *Convection oriented heat exchanger model*, IEEE International Conference on Control and Automation, ICCA **2016-July** (2016), 347–352.

[8] J. Paulo Garcîa-Sandoval, Víctor Gonzîlez-Álvarez, and Carlos Pelayo-Ortiz, *Robust continuous velocity control of convective spatially distributed systems*, Chemical Engineering Science **63** (2008), no. 17, 4373–4385.

[9] E.M. Hanczyc and A. Palazoglu, *Sliding mode control of nonlinear distributed parameter chemical processes.*, I&EC Research (1995).

[10] Joao O. Hespanha, *Linear Systems Theory*.

[11] I E Idelchik, *Handbook of hydraulic resistance (3rd edition)*, Washington (2006).

[12] J M Kay and Ron M Nedderman, *Fluid Mechanics and Transfer Processes*, 3 ed., Cambridge University Press, New York, 1985.

[13] Y. Li Perry, *Lecture notes of Advanced Control System Designo Title*, University of Minnesota (2006).

[14] William S Romoser, *3rd Edition*, (1997).

[15] Huilan Shang, J. Fraser Forbes, and Martin Guay, *Feedback control of hyperbolic distributed parameter systems*, Chemical Engineering Science **60** (2005), no. 4, 969–980.

[16] Hiroaki Shiobara and Noriyuki Hori, *Numerical exact discrete-time-model of linear time-varying systems*, 2008 International Conference on Control, Automation and Systems, ICCAS 2008 (2008), no. September, 2314–2318.

[17] Herbertt Sira-Ramirez, *[1992_2]_H.Sira-Ramirez_DSMC strategies in the regulation of nonlinear chemical process.pdf*, 1992, pp. 1–21.

[18] Jiří Valtr, *Mass Flow Estimation and Control in Pump Driven Hydronic Systems*, Diploma thesis, CTU in Prague, 2017.

Appendix A

Testbed adventures

During the development and running experiments on the testbed, several bugs and hardships appeared. Some of them are listed in this appendix due to their curiousness or because we found it helpful for our or someone else's later work.

A.1 Phantom non-linearity of mass flow problem

During the usage of testbed we always faced a problem with the pressure relief valve. This component didn't seal properly, which caused a loss of pressure in the system and consequently a presence of bubbles in the system. When an air bubble gets into the pump, it rapidly reduces it's ability of functioning and the produced head as well as the mass flow significantly decreases. Fig. A.1 depicts a difference between the correct operation and an operation with an air bubble. The deadzone and non-linearity is apparent.

A.2 Improper component selection

Not all the components chosen to be placed in the testbed were the right ones. Some of them have different characteristics than it is actually needed.

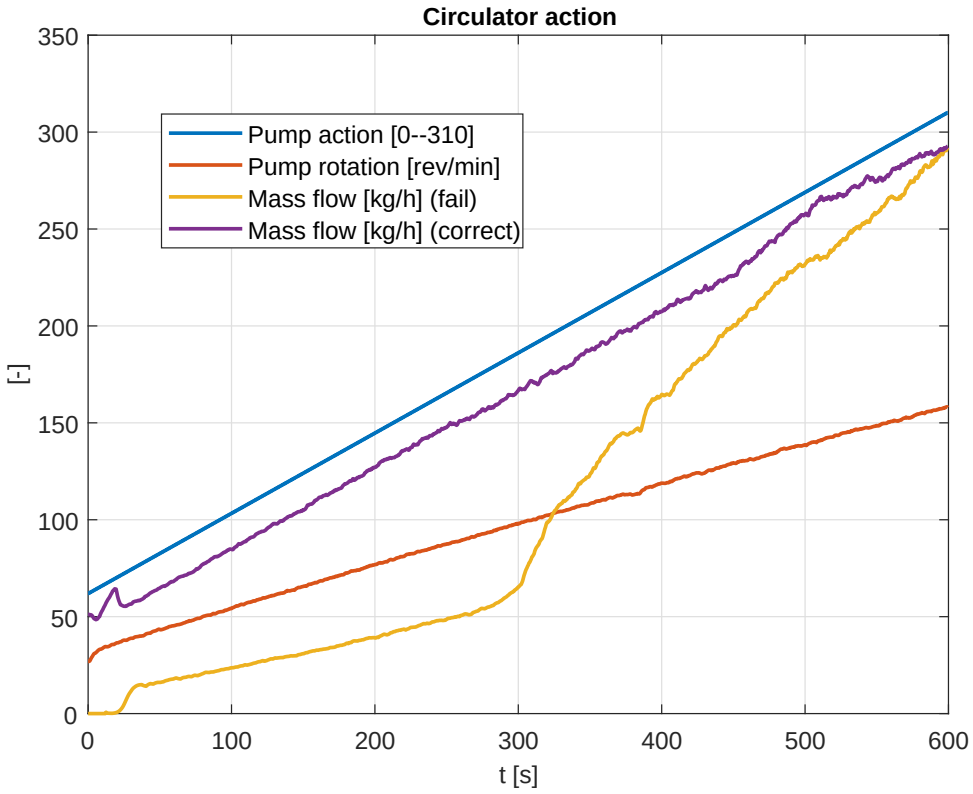

Figure A.1: Comparison of pump action and mass flow

Boiler & heat exchanger power

Even that the utilized boiler is marked with a sticker "Macedonia's Best Choice", for our testbed it wasn't the best choice. The boiler power is limited to 1000 W nominally, which is below the heat power of the heat exchanger. For higher heat flow demands the boiler is not able to supply the system with enough hot water. The solution would be to use more powerful boiler or to decrease the heat transfer coefficient of the heat exchanger by closing part of it, which is what we did.

Pump mass flow & flow-meter range

The pump used in the secondary circuit is supposed to produce mass flow up to 1500 $\mathrm{kg\,h^{-1}}$, under an assumption that it is connected to a tube with a really low hydronic resistance. It is not a case of our testbed though. In it the pump is able to reach maximal flow round 340 $\mathrm{kg\,h^{-1}}$, depending on the actual pressure in the system. The flow-meter was chosen to cover the pump datasheet mass flow range, but during the experiments we

found, that the lower bound of the flow-meter range $30\,\mathrm{kg\,h^{-1}}$ is too high and we were not able to measure the mass flow in a range needed for the low heat flows.

A.3 Construction mistakes

Several problems were caused by the lack of experiences with the pipe sealing. One of the mistake was the placement of the air release valve, which we first indeed placed to the vertically highest point of the testbed, but it was impossible to use it and not to wet the whole tubing around. So we added a tube element and turned the valve from horizontal to vertical position. It makes the manipulation much easier and the piece of tube works as a reservoir for the air bubbles.

Next, a pressure relieve valve installed is the cheapest one and causes a problem, so it turns out it was not a good choice. Or it is just bad luck, no one can know for sure from one sample. The pressure relief valve doesn't leak properly and the water spills drops all the time. The water reduction induces a pressure decrease, which allows air bubbles to move through the testbed and worsen the pump performance.

Another mistake was to trust the fittings supplied with the heat exchanger. For the pressure of 4 bar it was not able to hold the tube and our lab got flooded.

Appendix B

CD Content

A CD is attached to the printed version of this thesis. It contains an electronic version of this thesis.

Appendix C

Images References

- Fig. 2.1: http://douglinstedt.theworldrace.org
- Fig. 4.4: http://www.anchorpumps.com
- Fig. 4.5: http://leov.com
- Fig. 4.7: http://www.watercoolinguk.co.uk
- Fig. 4.8a: http://shop.watercool.de
- Fig. 4.8: https://smallformfactor.net
- Fig. 4.9: http://honeywell.com
- Fig. 4.10: http://www.conrad.com
- Fig. 4.11: http://www.instructables.com
- Fig. 4.12: http://www.ferro.pl